Deltares

Developing a clay erosion model for levee landside slopes in case of wave overtopping

Progress report 2024 Sito-PS Kennis voor Keringen DE1

Developing a clay erosion model for levee landside slopes in case of wave overtopping
Progress report 2024 Sito-PS Kennis voor Keringen DE1

Author(s)
Vera van Bergeijk

Developing a clay erosion model for levee landside slopes in case of wave overtopping
Progress report 2024 Sito-PS Kennis voor Keringen DE1

Client	Rijkswaterstaat Water, Verkeer en Leefomgeving
Contact	Myron van Damme
Reference	Sito-PS Kennis voor Keringen DE1
Keywords	Wave overtopping, clay erosion, Delfzijl, Polder2Cs, IJsselmeerdijk

Document control	
Version	1.0
Date	04-12-2024
Project nr.	11210371-014
Document ID	11210371-014-GEO-0001
Pages	47
Classification	
Status	final

Author(s)

	Vera van Bergeijk	

Summary

Erosion of the landside slope by overtopping waves is one of the main failure mechanisms of dikes leading to a flood. The erosion process of the clay liner on the landside slope is not fully understood and no adequately validated erosion model for clay erosion is available for dikes in the Netherlands. The goal of this research is to develop an erosion relation for clay erosion on the landside slope by wave overtopping representative for the dikes in the Netherlands. Such a relation provides the possibility to take this step in the failure path to flooding into account. This will lead to a less conservative and more accurate flood probability estimate, because currently the probability of a flood in case of wave overtopping in combination with a failed revetment is assumed to be one. and lacks the strength of the underlying clay layer.

The strength of the clay layer is described in a theoretical model. Important parameters in this model are two strength parameters: the erodibility coefficient and the critical shear stress. In this study, the erodibility coefficient and the critical shear stress are calibrated using large-scale wave overtopping tests with the Wave Overtopping Simulator. These parameters are related to how fast the clay erodes and the erosion threshold, respectively. The data of wave overtopping tests of three cases are used in this study: Delfzijl, Polder2Cs and IJsselmeerdijk. The calibrated erosion parameters are compared to the erosion parameters determined with small-scale erosion tests and the calibration results of previous studies.

The calibration results of the Delfzijl case and the Polder2Cs case show a similar range as previous studies on the clay erosion on the landside slope by overtopping and overflow (Van Hoven, 2014; Van Hoven, 2024). For these dikes, a typical range for the erodibility coefficient between $1x10^{-6}$ and $1x10^{-5}$ m^3/Ns is found for a critical shear stress of 0 – 60 Pa. The IJsselmeerdijk case resulted in a smaller erodibility coefficient as the result of the boulder clay that seems stronger than normal clay. As a next step, the contribution of the clay layer to the failure probability could be determined using these ranges for the erosion parameters.

No clear relationship between the erosion parameters based on the large-scale tests and the small-scale tests was found. The results of the Jet Erosion Tests (JET) show a large variation in erosion parameters and is therefore not a useful method to determine the erodibility of the clay cover for wave overtopping. The Erosion Function Apparatus (EFA) tests could potentially be used to find a relation with the large-scale overtopping tests. No relation could be determined based on the three case studies because they differ in clay type: clay (Delfzijl), clay with grass roots (Polder2Cs) and boulder clay (IJsselmeerdijk). Therefore, it is recommended to study the clay erosion process further for another case study including large-scale and small-scale tests.

Contents

1 Introduction

Wave overtopping and subsequent erosion on the landside slope is one of the main failure mechanisms of a dike. Overtopping waves flow over the dike crest and down the landside slope exerting a hydraulic load on the dike cover. Erosion of the dike cover starts when the load exceeds the strength of the cover. Typical Dutch dikes have a grass cover on top of a clay layer, and a core made of sand or clay. The erosion process by wave overtopping of these dikes starts with erosion of the grass cover (Figure 1.1). Next, the clay layer underneath will erode until the dike core and/or crest is reached. Once the dike crest is lowered due to erosion, the probability of flooding of the hinterland increases dramatically.

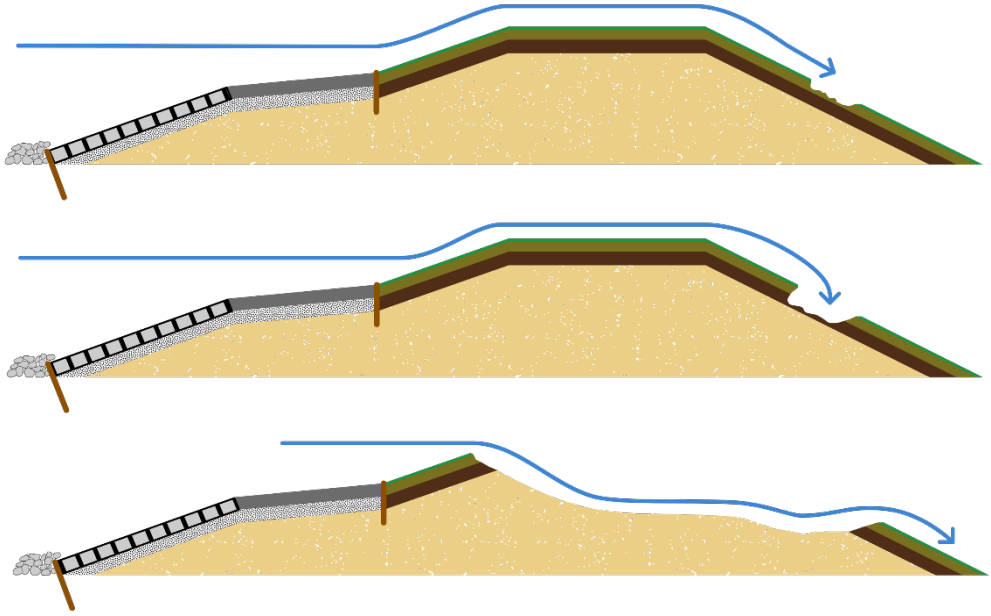

Figure 1.1 Example of the erosion processes leading to flooding: erosion of the grass cover, erosion of the clay layer and crest lowering. Figures made by Pieter van Geer (Koelewijn et al., 2024)

This study focuses on the second step of the erosion process: the erosion of the clay layer. Several formulas and models are available to describe this erosion process (Van Damme et al., 2023; Van Hoven, 2014). However, the values of the erosion parameters for clay erosion on the landside slope by wave overtopping are unknown for dikes in the Netherlands. The values found in literature are mainly related to overflow and show a large uncertainty.

The goal of this research is to develop an erosion relation for clay erosion on the landside slope by overtopping representative for the dikes in the Netherlands. Wave overtopping tests have been performed on the clay layer on the landside slope of the dikes in the Netherlands and Belgium to study this erosion process. The large-scale tests showed large differences in erosion rates. Hence, relatively large differences in erosion parameters are to be expected. An erosion model is used to calculate the observed erosion during these tests, where the test results are used to calibrate the erosion parameters in the model.

Additionally, small-scale erosion tests have been performed at the same locations of the overtopping tests. The results of the small-scale tests are compared to the large-scale tests. A relation between small-scale and large-scale tests makes it possible to determine the

erosion parameters for specific locations and clay types using cheaper small-scale methods instead of expensive and time-consuming large-scale overtopping tests.
A first step in this analysis was made in previous research (Koelewijn, 2024) for limited number of cases using the erosion model that was developed in the Polder2Cs project (Jellouli et al., 2023). No clear relation between the erosion parameters of the small-scale and large-scale test was found due to the large model uncertainty related to the translation of the wave conditions at the dike toe to the overtopping waves on the crest and the large number of input parameters with their own uncertainty. Therefore, it was recommended to study more cases using a simpler erosion model to reduce the number of input parameters and using the measured wave volumes on the crest as boundary condition to reduce the uncertainty in the model results.

In study, a simple erosion model is used to derive the erosion parameters for the wave overtopping tests performed at Delfzijl, Polder2Cs and the IJsselmeerdijk. This report is structures as follows: firstly, the erosion model is described in Chapter 2 together with a description of the calibration method. Chapter 3 provides information on the case studies and the results can be found in Chapter 4. The conclusions and recommendations are stated in Chapter 5.

2 Method

2.1 Erosion model

The erosion processes of the clay liner on the landside slope by overtopping waves consist of two phases (Figure 2.1). First, the erosion hole deepens leading to a hole with a cliff. During the second phase, the water will fall into the hole resulting in migration of the cliff towards the crest and simultaneously deepening of the erosion hole.

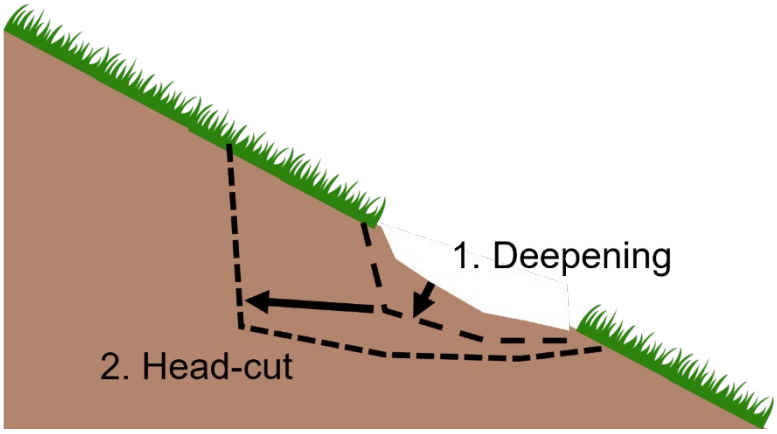

Figure 2.1 Visualisation of the erosion process of the clay liner by overtopping waves.

In this study two simple erosion models are used as recommended by Koelewijn (2024). The first erosion model is based on the description of the maximum load at the wave front and only describes the deepening of the erosion hole. The second erosion model describes the average load over the duration of the wave. This model calculates the erosion volume and can be applied to both erosion phases. However, the model has not been validated for head-cut erosion (Van Damme et al., 2023).

2.1.1 Maximum load formulation

Failure of the grass cover results in an erosion hole in the clay cover. Deepening of this erosion hole is described by the erosion rate E_r defined as the change of the erosion depth E_d over time.

$$E_r = \frac{\partial E_d}{\partial t} = K_d(\tau - \tau_c) \tag{2.1}$$

With:
E_r = erosion rate [m/s]
E_d = erosion depth [m]
t = time [s]
K_d = erosion coefficient describing the erodibility of the soil [m^3/Ns]
τ = shear stress [Pa]
τ_c = critical shear stress [Pa]

There are several formulations for the shear stress available. A simple description of the shear stress based on an equilibrium flow condition and the layer thickness is used in this study:

$$\tau = \rho g h_0 \sin(\alpha) \tag{2.2}$$

With:
ρ = density of water [kg/m^3]
g = gravitational acceleration (=9.81 m/s^2)
h_0 = layer thickness at the wave front on the crest [m]
α = angle of the landside slope [-]

This is a relatively simple description of the shear stress that does not include the change in the load over time or the change in load as result of the dike geometry, e.g. acceleration or deceleration along the slope or jet plunging in the erosion hole. This formulation is similar to previous studies for dikes in the Netherlands (Van Hoven, 2014; Van Hoven, 2022; Van Hoven, 2024). Based on literature values (NRCS, 1997) and back calculation of the Delfzijl wave overtopping test Van Hoven (2022; 2024) came to the following parameter characterisations:

- Critical shear stress τ_c: Uniform distribution between 0 and 60 Pa
- Erodibility coefficient K_d: Uniform distribution of log(K_d) between 10^{-5} and 10^{-7} m/s/Pa

2.1.2 Average load formulation

A formula was derived by Van Damme et al. (2023) to calculate the erosion volume based on the overtopping volume

$$E_{vol} = K_d \left(\frac{110}{3} \rho c_f V - \frac{8.8}{15} \tau_c^{3/2} \left(\rho c_f \right)^{-1/2} - 4.4 \tau_c V^{0.3} \right) \tag{2.3}$$

With:
E_{vol} = erosion volume [m^3/m]
c_f = friction coefficient [-], a value of 0.05 is used in this study
V = overtopping volume [m^3/m]

This formula is the result of an integration over time over Equation (2.1) and the use of empirical formulas (Equation (2.4)). Therefore, the coefficients have the following units: 110/3 m/s, 8.8/15 s^{-2} and 4.4 sm$^{-0.4}$. The time integration means that the hydraulic load in this formula describes the average load over the duration of one wave.

The main benefit of this formula is that the load is solely described by the overtopping volume. The overtopping volumes released during the large-scale wave overtopping tests are well documented. Therefore, the erosion volume during a test can easily be calculated using the cumulative overtopping volume. On the downside, the formulas in Equation (2.4) are specifically valid for volumes released by the (old) wave overtopping simulator and for the parameters on the crest. Additionally, the method does not take the increase in load due to head-cut formation into account.

2.2 Method

The erosion parameters are determined for three case studies: Delfzijl (1 test section), Polder2Cs (5 test sections) and IJsselmeerdijk (5 test sections). A detailed description of the case studies is provided in Chapter 3. This section describes the method to calibrate the

erodibility coefficient K_d using the maximum load formulation and the average load formulation.

The general idea of the wave overtopping simulator is that several water volumes are released on the dike crest and flow along the landside slope. The released volumes are representative for a storm with a significant wave height H_s and an average overtopping discharge q. The steering files of the tests contain the order and volumes of the released waves during the storm. The steering files are used as input for both methods.

Both erosion models contain two erosion parameters to calibrate: the critical shear stress and the erodibility coefficient. It should be noted that the calibrated erosion parameters are model-dependent due to the highly empirical nature of the models. The calibration results in several combinations of K_d and τ_c that correspond to the measured erosion. These combinations of K_d and τ_c are compared to the erosion parameters derived from the small-scale tests. Jet Erosion Tests (JET) and Erosion Function Apparatus (EFA) tests have been performed at the same locations as the wave overtopping tests. A detailed description of the small-scale test methods can be found in Van Damme et al. (2023).

2.2.1 Maximum load formulation

The hydraulic parameters are calculated for each overtopping volume using the empirical relations of Van der Meer et al. (2010) for volumes released by the (old) wave overtopping simulator at the dike crest:

$$\begin{aligned} h_0 &= 0.133V^{0.5} \\ u_0 &= 4.5V^{0.34} \\ T_0 &= 4.4V^{0.3} \end{aligned} \tag{2.4}$$

With:
u_0 = flow velocity at the wave front on the crest [m/s]
T_0 = overtopping period on the crest [s]

Next, the shear stress is calculated for every overtopping wave using Equation (2.2) . Equation (2.1) is discretised to calculate erosion depth during the test using the overtopping period as the time step of every wave:

$$E_d = \sum_i^N K_d(\tau_i - \tau_c) \cdot T_0 \tag{2.5}$$

With:
N = the number of overtopping waves during the test [-]
τ_i = shears stress of the i-th wave in the storm [Pa]

The erosion depth is calculated for several combination of K_d (1×10^{-8} to 1.2×10^{-4} m^3/Ns) and τ_c (0 – 200 Pa). Next, the combinations of K_d and τ_c resulting in the smallest error between the calculated erosion depth and the measured erosion depth during the test are selected.

2.2.2 Average load formulation

The erosion depth is a simple variable that is measured after every test. However, the erosion volume is only measured for a limited number of tests. In this study, the erosion volume [m^3/m] is derived from erosion profiles: the erosion volume is defined as the area between the reference profile and the profile measured after the test (Figure 2.2).

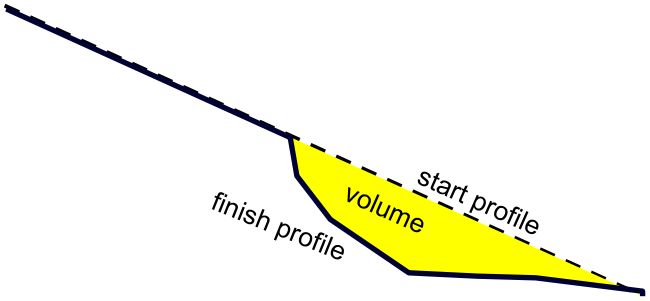

Figure 2.2 Calculation of the erosion volume from the erosion profiles

The cumulative overtopping volume V_{cum} is determined by a summation over all volumes released during the test. The erodibility coefficient $K_{d,j}$ after each test j is determined for three values of the τ_c (0, 30 and 60 Pa) using Equation (2.3)

$$V_{cum} = \sum_{i}^{N} V_i$$

$$K_{d,j} = \frac{E_{vol,j}}{\left(\frac{110}{3} \rho c_f V_{cum} - \frac{8.8}{15} \tau_c^{3/2} \left(\rho c_f \right)^{-1/2} - 4.4 \tau_c V_{cum}^{0.3} \right)} \tag{2.6}$$

With:
V_i = overtopping volume of the i-th wave in the storm [m^3/m]
$E_{vol,j}$ = erosion volume measured after test j [m^3/m]

The average erodibility coefficient $K_{d,mean}$ over the measurements is calculated. Additionally, the erodibility coefficient of the final measurement $K_{d,end}$ is reported because it is often more important to predict the final erosion volume instead of the intermittent erosion stages.

$$K_{d,mean} = \sum_{j}^{M} K_{d,j}$$

$$K_{d,end} = K_{d,M} \tag{2.7}$$

With:
M = total number of erosion measurements [-]

3 Overview case studies

3.1 Delfzijl

3.1.1 Wave overtopping experiments

Wave overtopping experiments on bare clay have been performed in the winter of 2006 and 2007 near Delfzijl (Akkerman et al., 2007). The dike at this location has a landside slope of 1:3. The upper 20 cm of the grass sod was removed by using two cranes with a digging bucket that was used as a 'knife' to cut the grass cover.

The initial wave overtopping tests with 0.1 l/s/m showed a 'roughening' of the surface of the clay with local small erosion pits, which might be the result of the grass removal method that was used. After these small initial waves, a 6-hour storm was simulated with an average wave overtopping discharge of 1 l/s/m executed in parts of 2 hours with measurements during the breaks. No significant erosion was observed during these test (Figure 3.1).

Next, a storm with an average wave overtopping discharge of 5 l/s/m volume was simulated for 6 hours with breaks every 2 hours. Two erosion trenches were formed during these tests (Figure 3.1). Finally, a storm with average wave overtopping discharge of 10 l/s/m was simulated, again for 6 hours with breaks every 2 hours. The progression of the erosion profile during the tests can be seen in Figure 3.2 (Akkerman et al., 2007).

Figure 3.1 Erosion during the Delfzijl tests after 2 hours of 1 l/s/m (left), 6 hours of 5 l/s/m (middle) and 6 hours of 10 l/s/m (right)

The maximum erosion depth, the erosion volume and the cumulative overtopping volume used as input for the calculations are summarized in Table 3.1. The maximum vertical erosion depth was reported in Koelewijn (2024). The erosion profiles were extracted from Figure 3.2 using a webplot digitalizer (Rohathi, 2024; Table B.2). The erosion volumes in m^3/m were calculated as the area between the reference profile after 6 hr of 1 l/s/m and the measured erosion profiles.

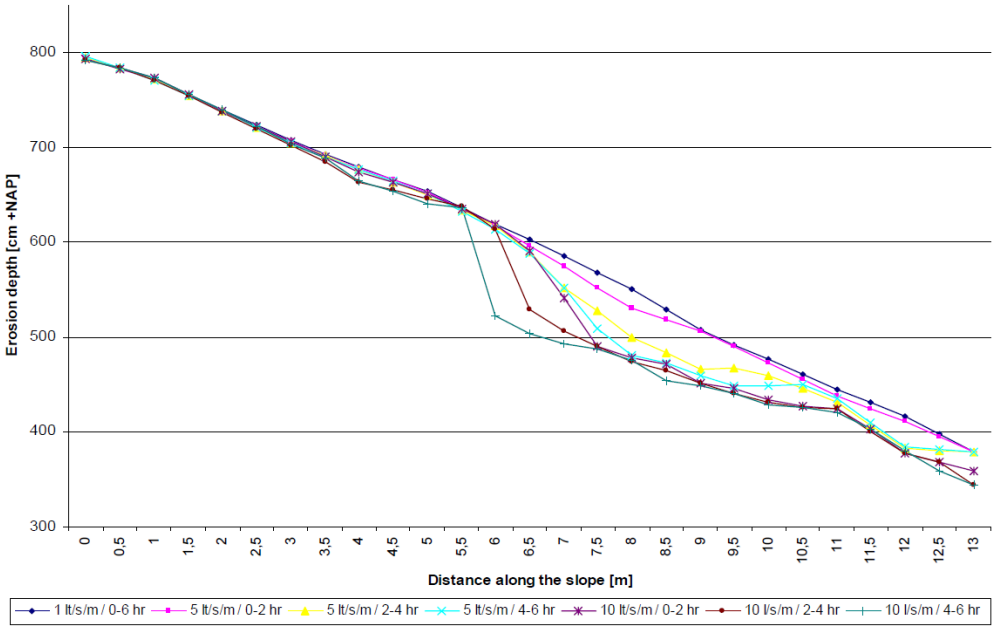

Figure 3.2 Measured erosion (highest values of both trenches) along the slope for the Delfzijl tests (Akkerman et al., 2007).

Table 3.1 Maximum recorded vertical erosion depths and the erosion volume of the maximum hole during the Delfzijl tests relative to the erosion after the 1 l/s/m test.

Test	Maximum vertical erosion depth [m]	Erosion volume [m3/m]	Cumulative overtopping volume [m3/m]
5 l/s/m after 2 hours	0.19	0.37	0.032
5 l/s/m after 4 hours	0.52	1.84	0.070
5 l/s/m after 6 hours	0.69	2.17	0.11
10 l/s/m after 2 hours	0.76	2.90	0.18
10 l/s/m after 4 hours	0.79	3.45	0.25
10 l/s/m after 6 hours	0.98	4.56	0.32

3.1.2 Small-scale tests

No small-scale erosion tests have been performed around the time of the overtopping tests in the winter of 2006/2007. Soil investigations were performed by Fugro in June 2004 and May 2006 and by GeoDelft in March 2007 (Akkerman et al., 2007).
For further research, samples were collected at Delfzijl in June 2023 for EFA tests (Bennabi, 2023; Koelewijn, 2024). The critical shear stress and the erodibility coefficient that were determined from these tests are summarized in Table 3.2.

Table 3.2 The critical shear stress τ_c and the erodibility coefficient K_d determined from the EFA tests on Delfzijl samples (Bennabi, 2023)

Sample	τ_c [Pa]	K_d [m^3/Ns]
1	0.6	6.4×10^{-8}
2	0.5	3.3×10^{-8}
3	0.1	9.6×10^{-8}
4	1.6	4.7×10^{-8}
6	0.7	8.8×10^{-8}

3.2 Polder2Cs

3.2.1 Wave overtopping tests

Wave overtopping tests were carried out on the landside slope of the dike along the Hedwigepolder in the Southwest of the Netherlands as part of the Interreg Polder2C's project in 2022 (Daamen et al., 2022; Ebrahimi et al., 2025; Van Damme et al., 2023). In total, five tests on bare clay were carried out, divided over two parts of the landside slope (slope steepness 1:2.6) as indicated in Figure 3.3. The upper 20 cm of the test section removed by an excavator, but it should be noted that root system of the grass cover in this case reached deeper than 20 cm (Koelewijn, 2024).

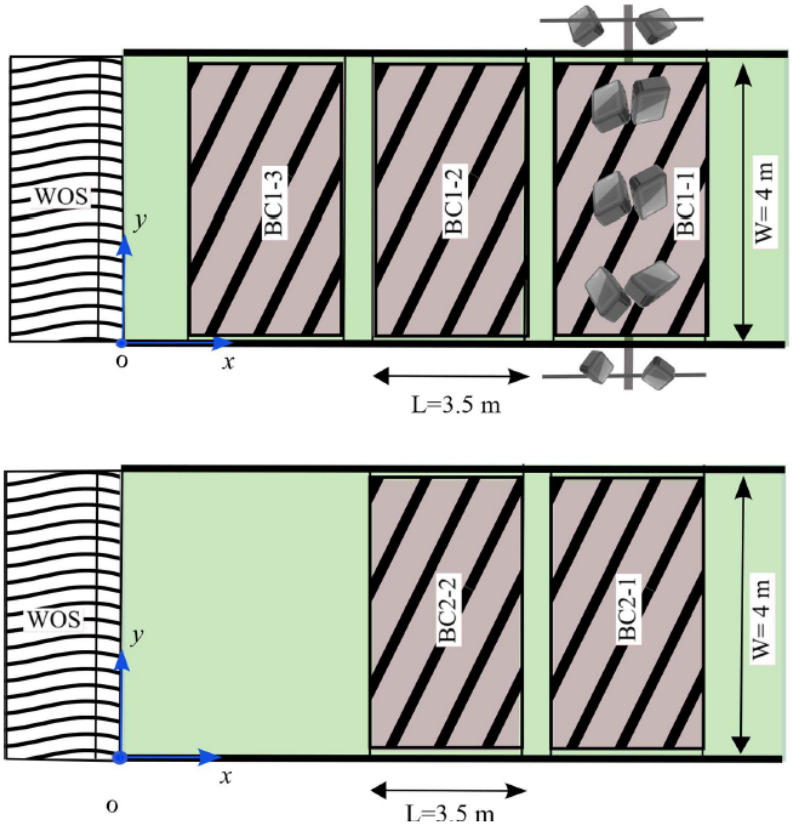

Figure 3.3 Schematic top view of tests on Bare Clay BC and the location of the Wave Overtopping Simulator WOS (Ebrahimi et al., 2024). Flow direction left (crest) to right (toe)

The first three tests were carried out on the part indicated by 'BC1' with regular waves (Figure C.1). The other tests were carried out on the part indicated by 'BC2' with a two-hour storm for river conditions (q = 60 l/s/m, H_s=0.5 m) and sea conditions (q = 50 l/s/m, H_s=1.0 m) (Figure C.2). The maximum erosion depth measured during the tests is reported in Table 3.3 and photos of the erosion holes of section BC2 are shown in Figure 3.4.

Table 3.3 The maximum erosion depth measured during the Polder2Cs tests (Ebrahimi et al., 2025)

Test	BC1-1	BC1-2	BC1-3	BC2-1	BC2-2
Maximum erosion depth [m]	0.64	0.36	0.34	0.75	0.55

Figure 3.4 Final situation at the end of test BC2_1 (Left) and BC2_2 (Right)

3.2.2 Small-scale tests

Five samples were taken for EFA tests close to the location of the wave overtopping tests a few weeks prior to the tests (Table 3.4). These EFA tests focussed on the initial erodibility and the low K_d values is probably related to the presence of roots in the samples (Koelewijn, 2024). Additionally, samples for the laboratory JET tests were taken from a larger part of the Hedwigepolder and the adjacent Prosperpolder (Table 3.5).

Table 3.4 Selection of information from the EFA results (Van Damme et al., 2023) with the critical shear stress τ_c and the erodibility coefficient K_d

Sample	Identification	τ_c [Pa]	K_d [m³/Ns]
1	Clay soil with roots	0.2	12.14×10^{-6}
2	Silty sand with roots and traces of rust	0.19	15.00×10^{-6}
3	Grey silt with roots and traces of rust	0.45	1.86×10^{-6}
4	Grey silt with roots	0.6	17.27×10^{-6}
5	Grey clay with roots	0.47	6.82×10^{-6}

Table 3.5 Selection of information from the JET results (Van Damme et al., 2023) with the critical shear stress τ_c and the erodibility coefficient K_d

Sample	τ_c [Pa]	K_d [m³/Ns]
SX_E1_A	63 36	110×10^{-6} 5.2×10^{-6}
SXI_E1_A	72	24×10^{-6}
SXII_E1_A	41 30	7.2×10^{-6} 0.82×10^{-6}

3.3 IJsselmeerdijk

3.3.1 Wave overtopping tests

Wave overtopping tests at the IJsselmeerdijk near Lelystad have been performed in September and Oktober 2023 (Daamen et al., 2024). At this location, the cover consists of boulder clay with an upper layer of 30 cm clay and a grass cover. These overtopping tests focussed on the strengthening the two transitions on the landside of the dike: the geometrical transition from the upper slope to the berm and the transitions between asphalt and grass at the road on the berm (Figure 3.5). The following strengthening measures were tested:

- Section 0: Reference section.
- Section 1: The geometrical transitions and the transition from asphalt to grass was reinforced with NovoCrete®.
- Section 2: The geometrical transition and upper slope were reinforced with compacted clay. The transitions from asphalt to grass was reinforced with “geknokte bermverbandblokken”.
- Section 3: The geometrical transition was smoothed to a curved radius and the transitions from asphalt to grass was reinforced with “opsluitband verankerd doorgroeibaar geogrid”.
- Section 4: Reference section.

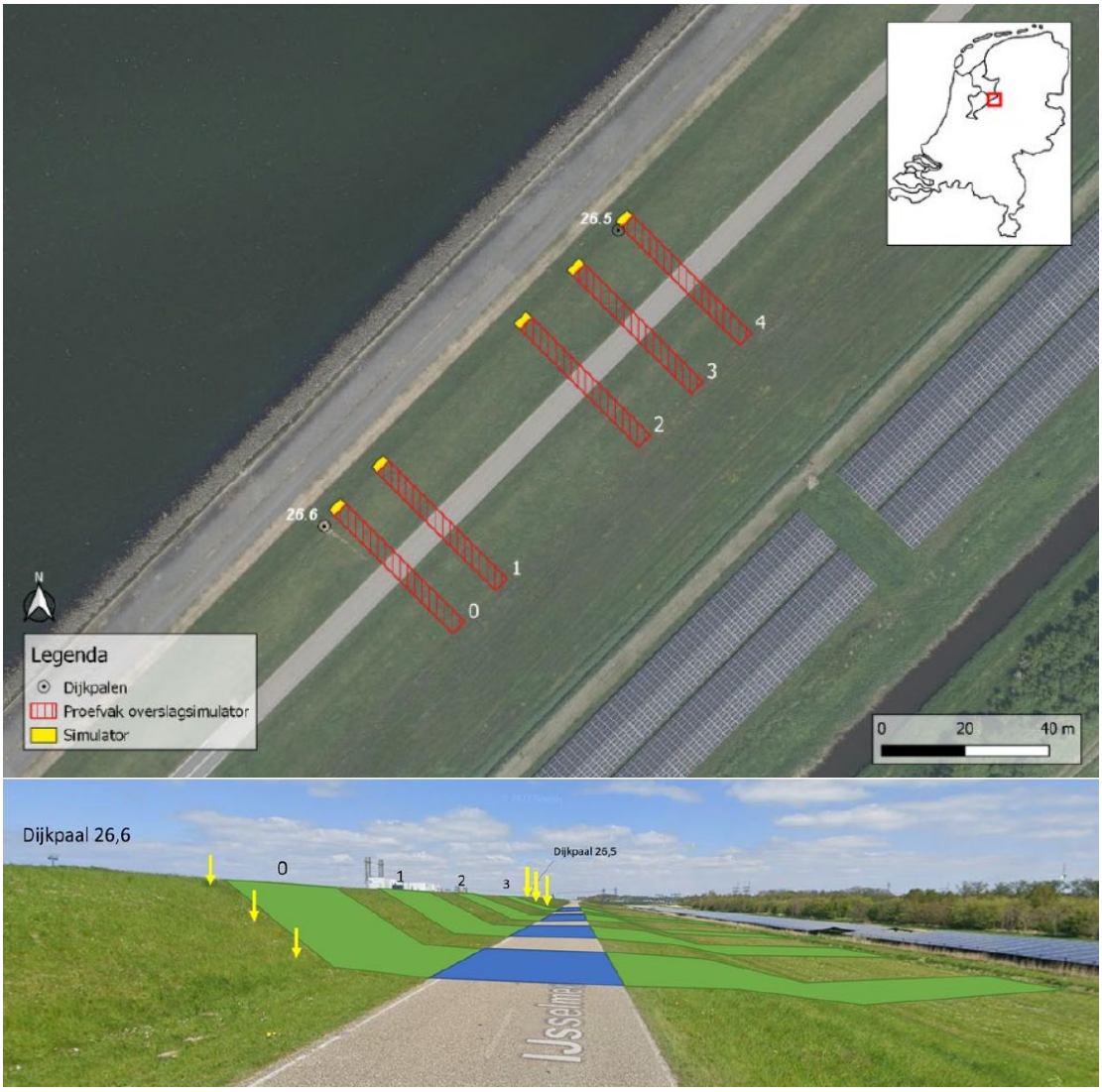

Figure 3.5 Locations of tests sections on the IJsselmeerdijk (top) and the locations of the small-scale tests samples indicated by the yellow arrows (bottom)

Contrary to the other two test cases, these wave overtopping tests have not been performed on bare clay but on both the grass and clay cover. This means that the calculations with the clay erosion model only start after grass cover failure. The erosion was measured approximately every hour during the overtopping tests and the moment of grass cover failure was determined by Daamen et al. (2024). The tests were carried out with overtopping discharges varying between 1 l/s/m and 100 l/s/m representative for the river regime

(H_s = 1 m, duration = 5 hr) and the lake regime (H_s = 3.2 m, duration = 6 hr). The steering files were provided by Daamen et al. (2024).

Three different clay types are tested as the result of the strengthening measures: boulder clay (reference sections), compacted clay (section 2) and recent applied clay in the arc radius (section 3). In this study, the critical shear stress and the erodibility coefficient is determined for the boulder clay and the compacted clay.

Most erosion occurred at the transition from the slope to the berm, where the load increases due to the change in slope angle. Due to the simplicity of the load description, it was decided to only include the erosion on the upper slope in this study. A negligible amount of erosion was observed for section 1. For the other four tests section, the erosion measurements were selected based on the following criteria: (1) erosion is on the upper slope and (2) at least one measurement of clay erosion (after grass cover failure) is available. The measured maximum erosion depth for the selected measurements are summarized in Table 3.6 (section 0), Table 3.7 (section 2), and Table 3.8 (section 4).

Table 3.6 Erosion measurements on the upper slope of reference section 0. The load is described by the discharge (wave height) with the discharge in l/s/m and the wave height in m.

Location	Maximum erosion depth [m]	Load	Comments
4A	0.28	1(1), 10(1)	Grass cover failure
	0.33	1(1), 10(1), 100(1)	
	0.55	1(1), 10(1), 100(1), 4.0 hours of 50(3.2)	Section was covered during the next tests
7B/8	0.22	1(1), 10(1), 100(1), 4.0 hours of 50(3.2)	Grass cover failure
	0.22	1(1), 10(1), 100(1), 50(3.2)	Grass cover failure
	0.80	1(1), 10(1), 100(1), 50(3.2),4.25 hours of 100(3.2)	A trench was formed

Table 3.7 Erosion measurements on the upper slope of section 2 with compacted clay. The load is described by the discharge (wave height) with the discharge in l/s/m and the wave height in m.

Location	Maximum erosion depth [m]	Load	Comments
10	0.27	1(1), 10(1),100(1)	Grass cover failure
	0.48	1(1), 10(1),100(1), 3.2 hours of 50(3.2)	
	0.55	1(1), 10(1),100(1),50(3.2)	
	0.60	1(1), 10(1),100(1),50(3.2), 2.0 hours of 100(3.2)	
	0.65	1(1), 10(1),100(1),50(3.2), 4.0 hours of 100(3.2)	
	0.65	1(1), 10(1),100(1),50(3.2), 100(3.2)	

Table 3.8 Erosion measurements on the upper slope of reference section 4. The load is described by the discharge (wave height) with the discharge in l/s/m and the wave height in m.

Location	Maximum erosion depth [m]	Load	Comments
10D	0.15	1(1), 10(1), 100(1),1.0 hours of 50(3.2)	Damage to the grass cover
	0.20	1(1), 10(1), 100(1),2.0 hours of 50(3.2)	Grass cover failure
	0.25	1(1), 10(1), 100(1), 50(3.2)	

Photogrammetry measurements were performed by the hydraulics group of UCLouvain at test section 2 with compacted clay (Daamen et al., 2024; Ebrahimi et al., 2024). The post-processing of the photogrammetry results produces erosion profiles at the location where maximum erosion occurred (Figure 3.6). According to Table 3.7, the grass cover failed after the tests with 100 l/s/m and H_s = 1m. Therefore, the profile 1m100lsm-2.5hr was used as a reference to determine the erosion volume in m^3/m. The cumulative overtopping volume was calculated using the remaining 2.5 hr of 100 l/s/m and the overtopping volumes released during the next tests (Table 3.9).

Table 3.9 The erosion volume of section 2 of the IJsselmeerdijk for compacted clay determined from the photogrammetry results of the hydraulics group of UCLouvain (Ebrahimi, 2024)

Test	Erosion volume [m3/m]	Cumulative overtopping volume [m3/m]
2 hours of 50 l/s/m with H_a = 3.2 m	0.75	1.27
6 hours of 50 l/s/m with H_a = 3.2 m	1.61	1.97
6 hours of 100 l/s/m with H_a = 3.2 m	2.31	4.13

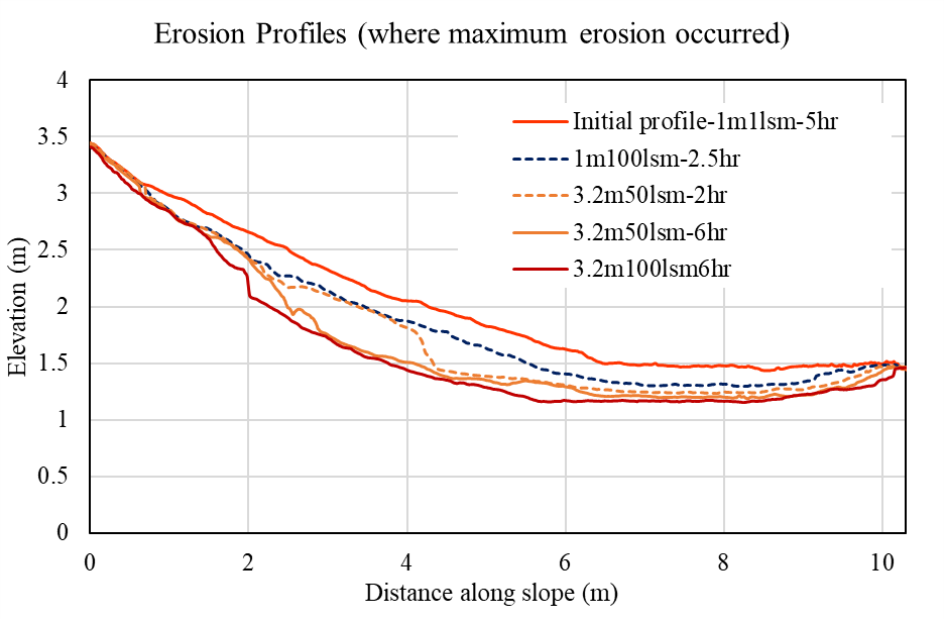

Figure 3.6 Post-processing of photogrammetry results performed by the hydraulics group of UCLouvain (Ebrahimi, 2024)

3.3.2 Small-scale tests

EFA tests were performed on 6 samples of the IJsselmeerdijk on the boulder clay of the reference situation (Figure 3.5). The derivation of the erodibility coefficient K_d from the EFA results are described in Appendix D. A detailed soil investigation was performed by Fugro that included JET tests. The results of the JET tests are summarised in Table 3.11.

Table 3.10 The critical shear stress τ_c and the erodibility coefficient K_d from the EFA tests of the IJsselmeerdijk on boulder clay (Appendix D)

Sample	Identification	τ_c [Pa]	K_d [m^3/Ns]
1	Silt soil with shells	0.50	0.099×10^{-6}
2	Sandy silt with shells	0.45	0.40×10^{-6}
3	Fine sand with chippings	1.65	0.023×10^{-6}
4	Fine sand with chippings	0.80	0.093×10^{-6}
5	Silt soil with chippings	0.65	0.056×10^{-6}
6	Silt soil with shells and roots	3.30	0.018×10^{-6}

Table 3.11 The critical shear stress τ_c and the erodibility coefficient K_d from the JET tests of the IJsselmeerdijk on boulder clay (Halter, 2024)

Sample	Depth (m)	Critical stress τ_c [Pa]	K_d [m^3/Ns]
MB03	0,85-0,95	67	4×10^{-6}
		8	0.15×10^{-6}
MB07	0,60-0,75	14	87×10^{-6}
		12	19×10^{-6}
		10	6×10^{-6}
MB08	0,65-0,80	94	77×10^{-6}
		9	22×10^{-6}

4 Results

4.1 Calibration results

4.1.1 Range critical shear stress

In previous studies, a range for the critical shear stress of 0 Pa – 60 Pa was established (Van Hoven, 2022; Van Hoven, 2024). The critical shear stress describes the erosion threshold: erosion occurs for shear stresses larger than the critical shear stress. An erosion threshold can be derived from the observation during the Delfzijl tests and the Polder2Cs tests.
No significant erosion was observed during the Delfzijl tests with 1 l/s/m, but these tests resulted in roughening of the surface. Erosion was observed during the Delfzijl tests with 5 l/s/m. This means that the erosion threshold for the Delfzijl case is between an average overtopping discharge of 1 l/s/m to 5 l/s/m. Multiple wave volumes were released since the tests were performed with irregular waves (Appendix B) leading to a range of shear stresses (Table 4.1). Therefore, it is difficult to determine a critical shear stress for the Delzijl case.

Observations during the Polder2Cs tests with regular waves showed that some erosion occurred even for the smallest wave volumes of 100 l/m, corresponding to a shear stress of 153 Pa. This observation was made in the short durations between two subsequent released wave volumes, which makes it difficult to estimate if this erosion was significant compared to the surface roughening during the Delfzijl tests. However, it is estimated that the critical shear stress is lower than 153 Pa for the Polder2Cs case.

For this study, the suggested range of 0 Pa – 60 Pa was used to derive the erodibility coefficient K_d, since the observations during the wave overtopping tests do not provide a clear range for the critical shear stress.

Table 4.1 The shear stress calculated for the overtopping volumes released during the Delfzijl test with 1 l/s/m

Volume [l/m]	Number in 6 hours	Shear stress [Pa]
50	54	97
150	54	168
400	9	275
700	6	363
1000	3	435

4.1.2 Delfzijl

4.1.2.1 Maximum load formulation

Calibration of the Delfzijl tests using the maximum load formulation results in multiple combinations of the erodibility coefficient K_d and the critical shear stress τ_c for each erosion measurement, which is visualized by the lines in Figure 4.1. The erosion measurement after 4 hours of 5 l/s/m results in the highest values of K_d and the final measurement after 6 hours of 10 l/s/m results in the lowest value. These tests result in the range of K_d for the critical shear stress of 0 Pa, 30 Pa and 60 Pa summarized in Table 4.2.

The value of the critical shear stress has a minor influence on the calibrated value of K_d, the variation is mainly the result of the variation between the tests. This variation could be an indication of the variability in clay strength, but it might also be related to the variability in the

location of the maximum erosion depth. These variations are partially balanced for longer test durations, as can be seen in the lines for 4 hr 10 l/s/m and 6 hr 10 l/s/m that are close together. Another possibility is the change in hydraulic load in the erosion hole as the result of head-cut formation, which is not included in the erosion model.

The EFA tests predict a lower erodibility coefficient compared to the calibration results.

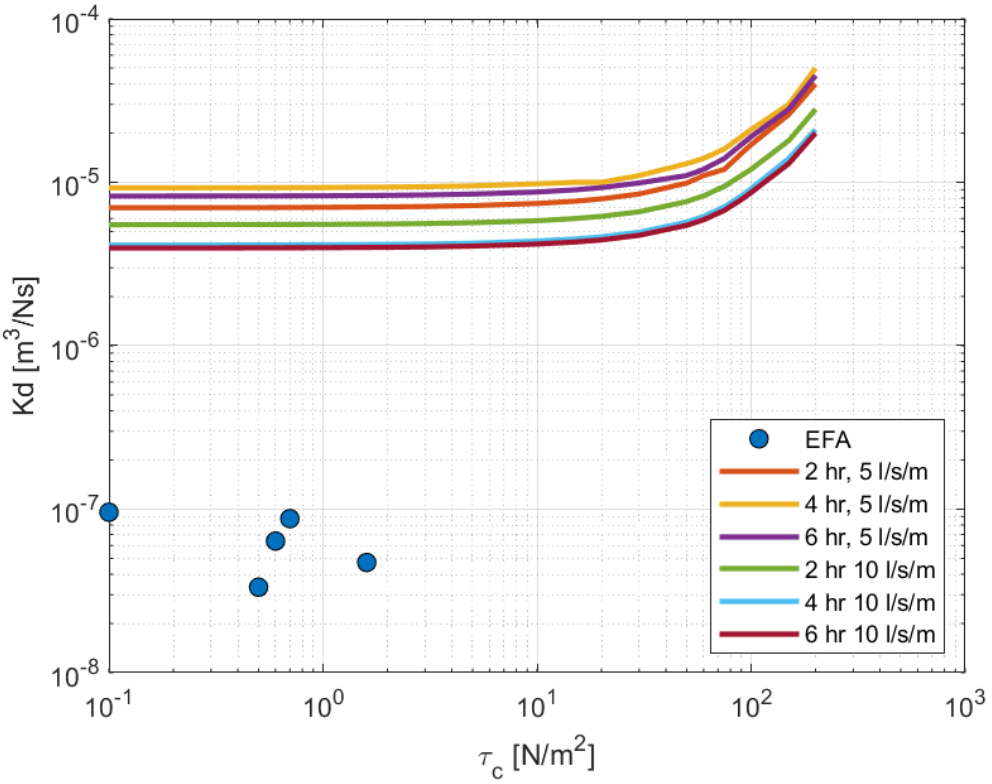

Figure 4.1 Combinations of the erodibility coefficient K_d and the critical shear stress τ_c corresponding to the measured maximum erosion depth of the Delfzijl tests together with the values determined with the EFA tests

Table 4.2 The calibrated erodibility coefficient K_d (m^3/Ns) for the three case studies using the maximum load formulation and the average load formulation

Case study	Method	τ_c = 0 Pa	τ_c = 30 Pa	τ_c = 60 Pa
Delfzijl	Maximum load	1.3 – 3.1 × 10^{-6}	1.5 – 3.7 × 10^{-6}	1.8 – 4.4 × 10^{-6}
	Average load	8.0 – 9.0 × 10^{-3}	0.9 × – 1.4 × 10^{-2}	1.0 – 1.9 × 10^{-2}
Polder2Cs	Maximum load – regular waves	0.9 – 2.9 × 10^{-6}	0.9 - 3.2 × 10^{-6}	1.0 – 3.4 × 10^{-6}
	Maximum load – irregular waves	5.7 – 6.2 × 10^{-7}	6.3– 6.9 × 10^{-7}	7.1 – 7.9 × 10^{-7}
IJsselmeerdijk	Maximum load – reference	0.2 – 2.8 × 10^{-7}	0.2 - 3.0 × 10^{-7}	0.2 – 3.2 × 10^{-7}
	Maximum load – compacted clay	0.8 – 2.5 × 10^{-7}	0.9 – 2.7 × 10^{-7}	1.0 – 2.9 × 10^{-7}
	Average load – compacted clay	3.1 – 3.6 × 10^{-6}	3.1 – 3.7 × 10^{-6}	3.2 – 3.9 × 10^{-6}

4.1.2.2 Average load formulation

The erodibility coefficient K_d is determined from a fit through the measured erosion volumes for a critical shear stress of 0 Pa, 30 Pa and 60 Pa (Figure 4.2). The erodibility coefficient determined using the average of the 6 measurements $K_{d,mean}$ is large compared to the erodibility coefficient of the final measurement $K_{d,end}$ (Section 2.2.2). This is because a relatively large erodibility coefficient is required to predict the first three measurements leading to an overestimation of the last three measured erosion volumes, especially for a high critical shear stress.

This is contrary to what is expected from the overtopping discharges during the tests: the first three erosion measurements are relates to the tests with 5 l/s/m and the final three measurements to 10 l/s/m. An increase in erosion volume is expected with an increase overtopping discharge. The decrease in erosion volume over time could be related to the soil structure, for example a top layer with a high erodibility and a bottom layer with a lower erodibility. Another explanation could be that the erosion hole affects the load (Van Bergeijk et al., 2022; Van Damme et al, 2023), which is not included in the erosion models in this study.

The erodibility coefficient determined using the average load formulation results in an erodibility coefficient that is 2 orders of magnitude larger than the maximum load formulation using the erosion depth (Table 4.2). As mentioned in Section 2.2, the erosion parameters are model-dependent and cannot be used for a different erosion model. Possible explanations for the difference between the erosion models are:

- Description of the load: the average load is lower compared to the maximum load formulation. This means that a higher erodibility coefficient is necessary for the average load description to predict the same amount of erosion as the maximum load description.
- Erosion measurements: the average load description is calibrated using the erosion volume while the maximum load description used the maximum erosion depth.

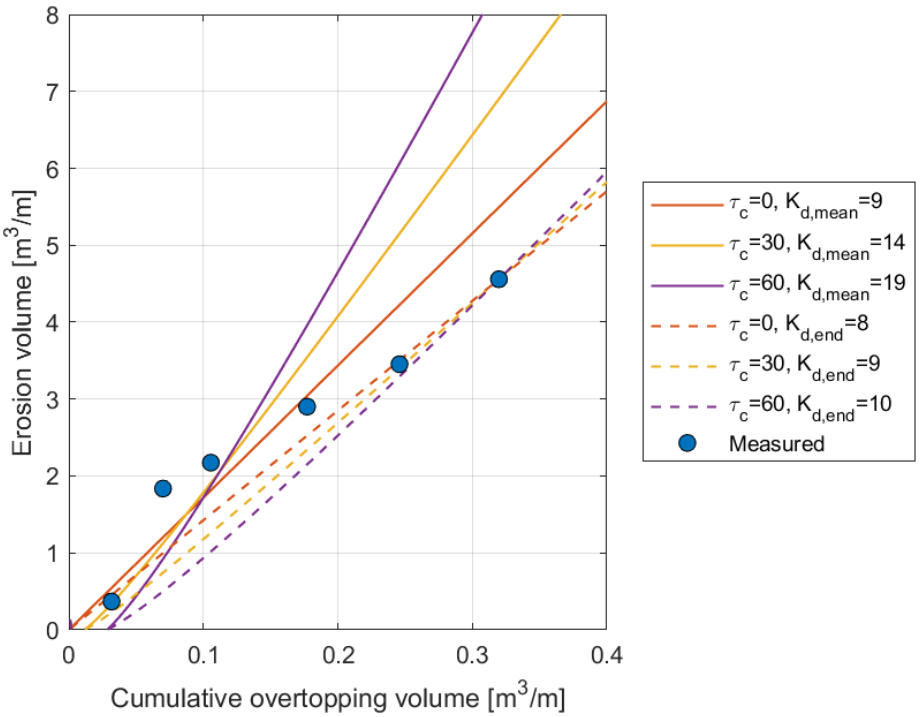

Figure 4.2 The erodibility coefficient K_d in 10^{-3} m^3/Ns and the critical shear stress τ_c in Pa determined from the measured erosion volume and the cumulative overtopping volume of the Delfzijl tests

4.1.3 Polder2Cs

The calibration results of the Polder2Cs tests together with the EFA and JET test results are shown in Figure 4.3. The calibration of the irregular wave tests (BC2-1 and BC2-2) lead to comparable results, however, the tests with regular waves (BC1-1 to BC1-3) predict a higher erodibility and show a larger spread. Therefore, the range of K_d for the critical shear stress of 0 Pa, 30 Pa and 60 Pa is determined for the irregular wave tests and the regular wave tests separately in Table 4.2. Again, the influence of the critical shear stress on the erodibility coefficient is small, especially for the regular waves.

The EFA tests predict a similar range of the erodibility coefficient as the calibration results. However, the EFA tests overestimate the erodibility coefficient compared to the calibration results of the irregular wave tests.

The calibration results fall within the range of the JET tests. The JET tests show a larger spread in the erodibility coefficient (2 orders of magnitude) for a small range of the critical shear stress.

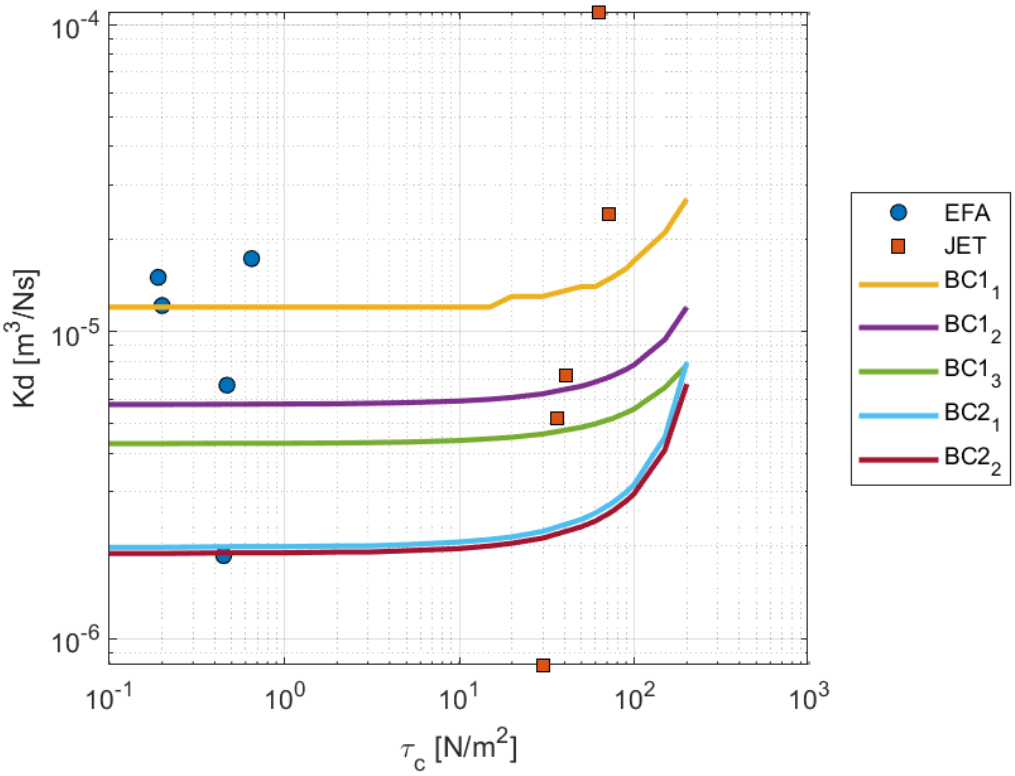

Figure 4.3 Combinations of the erodibility coefficient K_d and the critical shear stress τ_c corresponding to the measured maximum erosion depth of the Polder2Cs tests together with the values determined with the EFA tests and the JET tests

4.1.4 IJsselmeerdijk

4.1.4.1 Maximum load formulation

The calibration results of the reference section of the IJsselmeerdijk together with the EFA and JET test results are shown in Figure 4.4. The two reference sections (strook0 and strook4) give similar results. The erosion depth with the smallest overtopping discharge (100 l/n with H_s = 1m, Strook0 Vak4a) results in the lowest erodibility coefficient and the erosion depth measured after the highest discharge (100 l/s/m with H_s = 3.2 m, Strook0 Vak7B/8) results in the highest erodibility coefficient.

The JET tests and EFA tests have been performed on the boulder clay. The JET tests show a large spread in the erodibility coefficient of more than 9 orders of magnitude (10^{-7} to 10^{2}), while the EFA tests show a small under prediction of the calibration results.

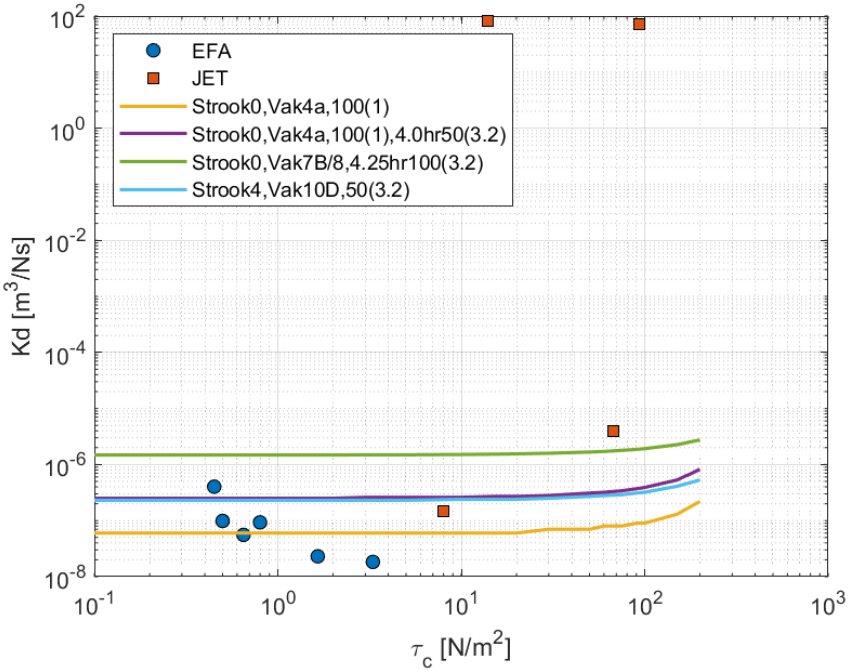

Figure 4.4 Combinations of the erodibility coefficient K_d and the critical shear stress τ_c corresponding to the measured maximum erosion depth of the IJsselmeerdijk tests of the reference sections with boulder clay together with the values determined with the EFA tests and the JET tests

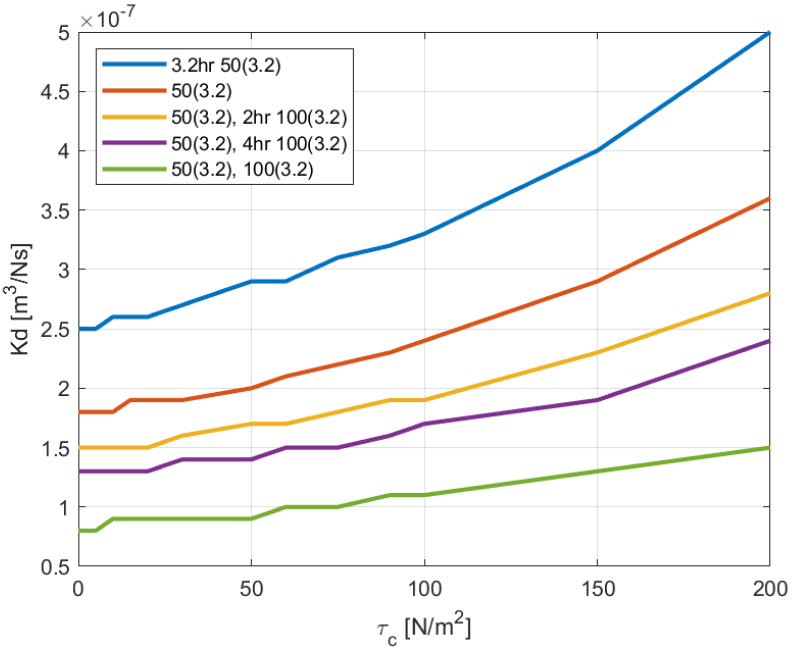

Figure 4.5 Combinations of the erodibility coefficient K_d and the critical shear stress τ_c corresponding to the measured maximum erosion depth of the IJsselmeerdijk tests of section 2 with freshly compacted clay

The erodibility coefficients calibrated for the test section with freshly compacted clay decrease with an increase in test duration and load (Figure 4.5). However, the variation between the test results is small, but looks visually larger because the plot does not include any small-scale test results. The erodibility coefficient of the compacted clay is similar to erodibility of the boulder clay of the reference sections (Table 4.2).

4.1.4.2 Average load formulation

The erodibility coefficient K_d for the freshly compacted clay is also determined using the average load formulation. The erodibility coefficient K_d determined from a fit through the measured erosion volumes shows only a small influence of the critical shear stress (Figure 4.6). This is probably related to the high overtopping discharge resulting in high hydraulic loads. This means that the erosion threshold is exceeded substantially by the majority of the waves and therefore has a minor influence on the erosion.

Similar to the Delfzijl case, the erodibility coefficient determined using all the measurements $K_{d,mean}$ is larger compared to only using the final measurement $K_{d,end}$. The erodibility coefficient determined using average load formulation results in an erodibility coefficient that is around 1 order of magnitude larger than the maximum load formulation (Table 4.2).

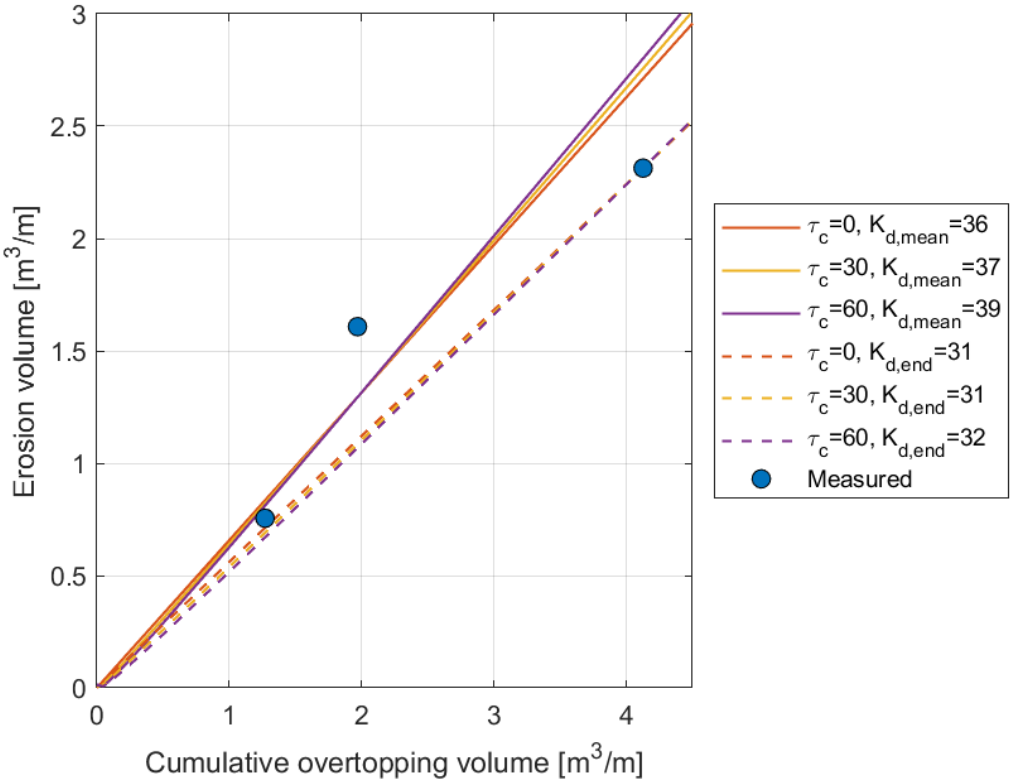

Figure 4.6 The erodibility coefficient K_d in 10^{-5} m^3/Ns and the critical shear stress τ_c in Pa determined from the measured erosion volume and the cumulative overtopping volume of the IJsselmeerdijk tests with freshly compacted clay

4.2 Comparison between large-scale and small-scale test methods

The goal of this study is to derive an erosion relation for Dutch dikes consisting of set of calibrated erosion parameters and an erosion model. A relation between the erodibility determined by small-scale tests and large-scale tests would be useful, so that the small-scale tests can be used for an estimate of the erosion parameters instead of expensive large-scale tests. The following conclusions can be drawn from the comparison between the calibration

results of the large-scale wave overtopping tests and the small-scale EFA and JET test per case study in the previous section.

First, the JET tests results in a large variation in the erodibility coefficient. This spread is so large that the large-scale erosion parameters will fall within the range of JET results. This means however that the JET tests are not useful to determine the erosion parameters for this application since the large spread in erosion parameters results in an unwanted large variation in possible erosion depths. Similar results were found for erosion on the outer slope by wave attack (Klein Breteler, 2024): the variation in measurements results was also large and therefore the results fell in multiple erosion categories. There was not clear relation between the erodibility determined from the JET measurements and the erosion measurements in the Delta Flume the large-scale wave flume of Deltares.

The EFA tests results compare better to the large-scale calibration results based on the maximum load formulation. The EFA tests show a similar magnitude to the calibration results of the Polder2Cs and IJsselmeerdijk results. The EFA tests at Polder2Cs show a similar range as the calibration erosion parameters for all tests, and a small overestimation compared to the calibrated erodibility for the irregular wave tests only. The EFA tests slight underestimate the erodibility coefficient for boulder clay calibrated using the reference section of the IJsselmeerdijk. The EFA results underestimate the erosion parameters for the Delfzijl case, but this could be due to the fact that the samples for the EFA tests were collected more than 16 years later and during very dry summer conditions. The samples are not saturated beforehand but put to the test as the samples come in.

Based on the calibration results with the maximum load formulation, the tested clay types ranking based from low to high erodibility would be: (1) IJsselmeerdijk (boulder clay of the reference clay and freshly compacted clay), (2) Polder2Cs and (3) Delfzijl. However, the ranking based on the EFA test would be different due to the Delfzijl results that differentiate from the large-scale tests (Figure 4.7).

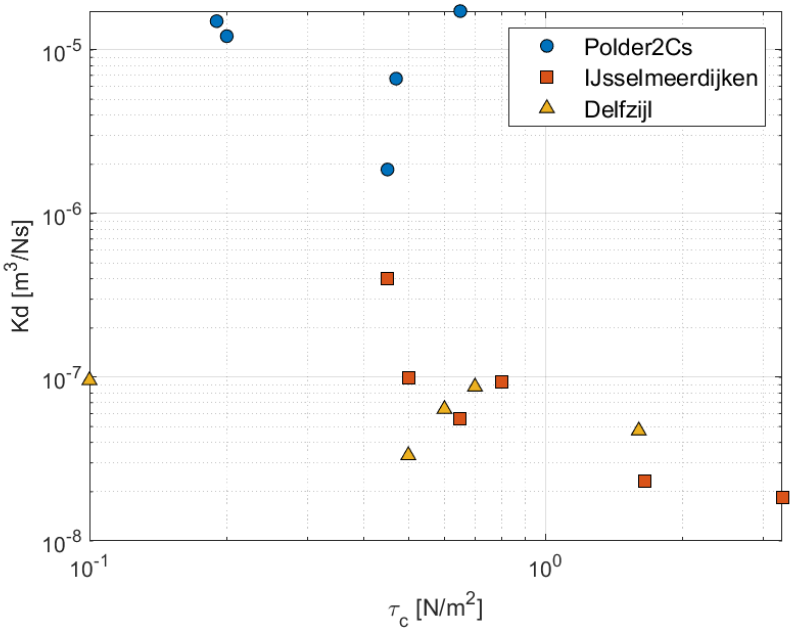

Figure 4.7 Comparison of the erosion parameters determined with the EFA tests for the three cases.

It is challenging to find a relation between the small-scale and large-scale tests because of the following explanations:

- The samples for the small-scale tests are collected at different depths than the erosion depths resulting during the wave overtopping tests. The erosion characteristics of the clay can change with depth, for example the IJsselmeerdijk where the lower clay layer consists of boulder clay.
- Difference in timing and conditions (e.g. moisture content) between the collection of samples and the execution in overtopping tests. An extreme example is the timing difference of 16 years for the Delfzijl case, but also difference between dry summer conditions and wet winter conditions.
- Difference in clay types between the case study: different behavior is expected for different clay types and therefore a different erosion relation. The case studies include two main exceptions: boulder clay for the IJsselmeerdijk and clay with grass roots for Polder2Cs.
- Differences in erosion scale: The samples in the small-scale methods are tested on the order of mm-cm's, while large-scale tests cover all processed from mm to dm's.
- Differences in loading conditions, both in scale and in mechanisms: During EFA tests a constant flow rate is applied, and a small water jet is used in the JET tests.
- Difference in time scale: The duration of overtopping tests is several hours, while the maximum duration of an EFA test is 30 minutes.

Overall, the EFA tests show promising results compared to the maximum load formulation.

Further optimalization of the description of the shear stress is possible such as increase in the load due to acceleration or deceleration along the slope or a jet plunging in the erosion hole. Three different formulations were tested in Appendix A that did not result in a better comparison with the EFA tests. It is recommended to first collect more measurements – combinations of both small-scale and large-scale tests - before a detailed study in the description of the shear stress is performed. This is also the case for the erosion volume method, for which only EFA tests are available for Delfzijl case and therefore no relation can be derived.

4.3 Comparison to other studies

The erodibility coefficient calibrated using maximum load formulation is compared to the erodibility coefficient found in previous studies for locations in the Netherlands (Table 4.3). Van Hoven (2014, 2024) used a similar method as the maximum load formulation to derive the erodibility coefficients, however, the shear stress above the critical value is integrated in Van Hoven (2014, 2024).

A different erodibility coefficient was found for the Delfzijl case by Van Hoven (2014), because the erodibility coefficient was determined using the average erosion rate of 0.097 m/hr during the 5 l/s/m. However, this value differs from the average erosion rate of 0.116 m/hr that can be derived from the measured erosion depth in Table 3.1.

The erodibility coefficient for the IJsselmeerdijk is smaller than the other locations. This is further supported by the large overtopping discharges that were required to erode the material. This could be related to the geometry where only the upper slope was included and therefore limited acceleration along the slope leading to smaller load. Other explanations could be the presence of the grass cover or a larger strength of boulder clay.

It is concluded from this study and Van Hoven (2024) that an erodibility coefficient of $1x10^{-6}$ to $1x10^{-5}$ in combination with a critical shear stress of 0 – 60 Pa could be used as a

typical range for dikes in the Netherlands. This range is only valid for the erosion model based on the maximum load formulation.
Van Hoven (2022; 2024) used a normal distribution for the erosion parameters (Section 2.1.1). The problem with an uniform distribution is the hard cut off at the boundaries, which means that the lower limit and upper limit need to be well known. It is recommended to further investigate the distribution type for the erosion parameters for probabilistic computations, although it is acknowledged that this might be a challenge due to the limited data.

Table 4.3 Comparison of the erodibility coefficient K_d for different locations in the Netherlands combined with the maximum load formulation

Study	Location	K_d (m^3/Ns)
Van Hoven (2014)	Delfzijl	$1.5x10^{-5}$ to $3.5x10^{-5}$ *
Van Hoven (2024)	Hollandsche IJssel HM 30,2	$1x10^{-6}$ to $3x10^{-6}$
	Hollandsche IJssel HM 33,8	$3x10^{-6}$ to $1x10^{-5}$
	Hollandsche IJssel HM 34,7	$1x10^{-6}$ to $2x10^{-6}$
	Hollandsche IJssel HM 38,4	$2x10^{-6}$ to $5x10^{-6}$
	Lekdijk centrum Krimpen	$4x10^{-7}$ to $2x10^{-6}$
This study	Delfzijl	$1.4x10^{-6}$ to $4.4x10^{-6}$
	Polder2Cs	$5.7x10^{-7}$ to $3.4x10^{-6}$
	IJsselmeerdijk	$2x10^{-8}$ to $3.2x10^{-7}$

* upper limit for τ_c = 40 Pa

5 Conclusions and recommendations

5.1 Conclusions

The erodibility coefficient and the critical shear stress for clay erosion on the landside slope are calibrated based on large-scale wave overtopping tests. The calibrated erosion parameters are compared to the erosion parameters determined with small-scale erosion tests and the calibration results of previous studies.

The erodibility coefficient was determined using two different erosion models: the maximum load formulation for deepening of the erosion hole and the average load formulation for the erosion volume. The calibrated erodibility coefficient is model-dependent; the erodibility coefficient of the average load formulation is 1 – 2 orders of magnitude larger compared to the maximum load formulations. This could be explained by differences in the load description and the erosion process in the models.

The calibration results of the wave overtopping tests showed that the critical shear stress has a minor influence on the erodibility coefficient. The variation in the calibrated erodibility coefficient is mainly caused by the variation between consecutive tests and erosion measurements. This variation is probably the result of the variability in clay strength and the variability in the location of the maximum erosion depth.

Comparison with the small-scale test methods indicated that the EFA method could potentially be used to find a relation with the large-scale overtopping tests. A relation could not be found for the case studies, because all three case studies seem to be an exception:

- The samples for the EFA tests at Delfzijl were collected more than 16 years after the overtopping tests in very dry summer conditions.
- The overtopping tests in the Polder2Cs project were performed on clay still containing a large number of grass roots that increases the erodibility significantly.
- The IJsselmeerdijk contains a layer of boulder clay underneath the upper clay layer. The erodibility properties of boulder clay are different from usual/ typical clay liners. Boulder clay consists more of silt than clay particles, but if applied correctly, maintains high strength properties due to large over-consolidation in undisturbed lumps.

The JET method results in a large range of the erodibility coefficient which makes it not a useful method to determine the erodibility of the clay cover for wave overtopping. The results show a large erodibility variation on a very small scale. The translation of (many) JET tests to bulk erosion parameters could possibly be established but this will be challenging and is beyond the scope of the current study.

The calibration results of the Delfzijl case and the Polder2Cs case coincide another study on the clay erosion on the landside slope by overtopping and overflow (Van Hoven, 2024). For these dikes, a typical range for the erodibility coefficient between $1x10^{-6}$ and $1x10^{-5}$ m^3/Ns is found for a critical shear stress of 0 – 60 Pa. This range is only valid for the shear stress based on an equilibrium flow condition and the layer thickness. The IJsselmeerdijk case resulted in a smaller erodibility coefficient as the result of the boulder clay that seems stronger than normal clay.

5.2 Recommendations

The main recommendation is to study the effect of clay erosion on the landside slope by overtopping waves on the failure probability using the simple erosion model and the erosion parameters determined in this study. This could provide insights in the contribution of the clay layer to flood safety compared to the grass cover. Additionally, a sensitivity study could help to determine which parameter has the main influence on the failure probability and for which parameters it is useful to reduce the uncertainty.

Next, it is recommended to perform more wave overtopping tests with clay erosion. These tests do not necessarily need to be performed on bare clay, but at least two erosion measurements after grass cover failure are required for the calibration study. The following measurements are recommended in combination with the wave overtopping tests:

- Perform EFA tests: collection of the samples should be around the same time as the wave overtopping tests. It is also recommended to collect the samples at different depths to determine if the strength changes with depth.
- A relation between small-scale tests and large-scale tested is also studied for clay erosion on the outer slope by wave attack (Klein Breteler, 2024; Zwanenburg et al., 2024). It is recommended to perform the same small-scale tests to determine if the erodibility of clay for wave attach and for wave overtopping can be quantified similarly.
- It is recommended to further investigate the distribution type for the erosion parameters for probabilistic computations.

References

Akkerman, G.J., van Gerven, K.A.J., Schaap, H.A., & van der Meer, J.W. (2007) Workpackage 3: development of alternative overtopping-resistant sea defences, phase 3: wave overtopping erosion tests at Groningen sea dyke, final report ComCoast WP3-16, 9R9112.B0/R/401070/Nijm, Royal Haskoning, Nijmegen, 21 September 2007

Bennabi, A. (2023) EFA erosion testing on soil samples from Delfzijl.

Bennabi, A. (2024) EFA tests on clay-samples ZZL. ESTP file number DS 012008

Daamen, E., Heida, L., & Mom, R. (2022), Factual report golfoverslag- en grastrekproeven Polder2C's (in Dutch), project number 20i830, version 3.0 (final), Infram Hydren, Maarn, 19 July 2022.

Daamen, E., Mom, R., & Wauben, C. (2024) Factual Report Erosiebestendigheid van Overgangen (in Dutch), project number 23i712, version 3.0 (final), Infram Hydren, Maarn, 3 March 2024

Ebrahimi, M., van Damme, M., van Hemert, H., & Soares-Frazão, S. (2025). Close-Range Photogrammetry Application to Monitor Levee Erosion in Case of Wave Overtopping. Journal of Hydraulic Engineering, 151(1), 04024057.

Ebrahimi, M., & Soares-Frazão, S. (2024). Spatial-temporal levee erosion and wavefront velocity dataset from in-situ wave overtopping experiments. Manuscript in preparation. UC Louvain.

Halter, W. (2024). Overslagproeven IJsselmeerdijk bij Lelystad. Analyse grond- en laboratoriumonderzoek (concept). Fugro 6423-228684.M01. 17 January 2024

Jellouli, M., Alleon, C., Neuts, A., Koelewijn, A. & van Damme, M. (2023) Erosion by overtopping flow, Code computation: OTE2CISL, Technical Notice, Polder2C's, August 2023

Klein Breteler, M. (2024) Onderzoeksprogramma Erodeerbaarheid klei op dijken. Kwantificering erodeerbaarheid met resultaten eenvoudige proeven. Deltares concept report 11206993-004-HYE-0019. 25 September 2024

Koelewijn, A. (2024). Dike erosion landside slope. Progress report 2023 Sito-PS KvK DE1. Deltares report 11210371-014-GEO-0001, 12 April 2024

Koelewijn, A., Van Geer, P., & Zwanenburg, S. (2024) Raamwerk voor analyse overstromingskans dijkerosie. Update 2023. Deltares concept 11210371-014-GEO-0001.

NRCS (1997) National Engineering Handbook part 628 Dams. Chapter 51 Earth Spillway Erosion Model and Chapter 52 Field Procedures Guide for the Headcut Erodability Index. Natural Resources Conservation Service. 210-vi-NEH. August 1997.

Rohathi, A., (2024) WebPlotDigitalizer. https://automeris.io, version = 5.2, accessed on 24 Oktober 2024

Van Damme, M., Alleon, C., Neuts, A., Koelewijn, A., Bennabi, A., Ebrahimi, M., Soares-Frazao, S., Sergent, P., & Samoui, H. (2023), Modelling erosion progression for steady overflow and wave overtopping conditions, Polder2C's report, 10 February 2023

Van der Meer, J. W., Hardeman, B., Steendam, G. J., Schüttrumpf, H., & Verheij, H. (2010). Flow depths and velocities at crest and landward slope of a dike, in theory and with the wave overtopping simulator. Coastal Engineering Proceedings, 1(32), 10.

Van Bergeijk, V. M., Warmink, J. J., & Hulscher, S. J. (2022). The effects of transitions in cover type and height on the wave overtopping load on grass-covered flood defences. Applied Ocean Research, 125, 103220.

Van Hoven, A. (2014) Residual dike strength after macro-instability. WTI 2017. Deltares 1207811-013-HYE-0001. 2 April 2014

Van Hoven, A. (2022) Kennis voor keringen GEKB Overgangen en objecten. Deltares 11208057-012-GEO-0001. 19 December 2022

Van Hoven, A. (2024) Stabiliteit bij golfoverslag. Postdictie erosie kleikern Hollandsche IJsseldijk 1953. Deltares concept report 11208415-007-GEO-0001

Zwanenburg, S., & Klein Breteler, M. (2024) Handreiking erosie van klei in golfaanval. Samenvatting van resultaten van het Onderzoeksprogramma Erodeerbaarheid Klei. Deltares concept report 11206993-004-HYE-0018

A Sensitivity analysis shear stress

A simple formulation of the shear stress is used in this study similar to previous studies. Three different formulations for the shear stress are studied to tests their performance in the erosion model (Equation (2.1)). The performance is studied qualitatively for the Delfzijl case to see if (1) the lines of the different tests coincide and thereby reduce the uncertainty in the calibration results, and (2) the calibration results show a better agreement with the EFA tests.

The first formulation (Figure A.1) is a small adaptation to Equation (2.5) where the time step is simplified from the overtopping period to 1 s

$$E_d = \sum_i^N K_d(\tau_i - \tau_c) \text{ with } \tau_i = \rho g h_{0,i} i \tag{A.1}$$

The second formulation (Figure A.2) uses the flow velocity on the crest (Equation (2.4)) to calculate the shear stress.

$$\tau = 0.5 f \rho g u_0^2 \tag{A.2}$$

The erosion depth is calculated using Equation (2.5).

Thirdly, the shear stress formulation (Figure A.3) developed in the Polder2Cs project (Van Damme et al., 2023; Jellouli, 2023) is tested:

$$\tau = \alpha \rho g h_c \left(\frac{E_d}{h_c} \right)^{0.582} \tag{A.3}$$

With:
α = coefficient for the effective stress due to plugging flow [-]. Default is 0.011.
h_c = critical depth of the flow [m]
E_d = erosion depth [m]

The critical depth h_c is calculated using

$$h_c = \left(\frac{q_{max}^{\ 2}}{g} \right)^{1/3} \text{ with } q_{max} = h_0 u_0 \tag{A.4}$$

Since the shear stress depends on the erosion depth, the erosion depth is calculated for every overtopping wave and used as input for the next wave. The erosion depth at the start of each test is set to 15 cm corresponding to the failure definition of the grass cover. The formulation is very sensitive for the value of the critical shear stress (Figure A.3).

The calibration results of the first two formulations are similar to the results in Figure 4.1. The magnitude of the erodibility coefficient depends on the shear stress formulation, but overall, the formulations show a similar performance. The Polder2Cs formulation is very sensitive for the value of the critical shear stress and resulting (Figure A.3).

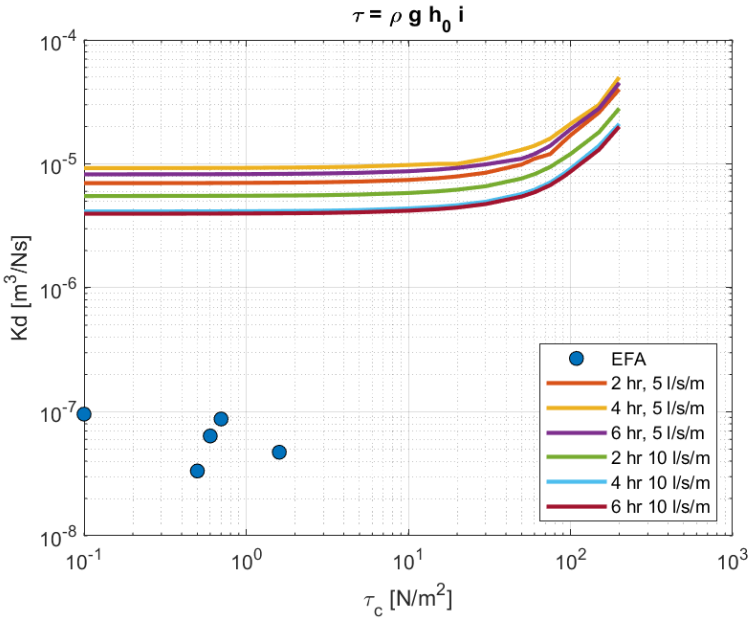

Figure A.1 Calibration results of the Delfzijl tests using $\tau=\rho g h_0 i$ and Δt = 1 s.

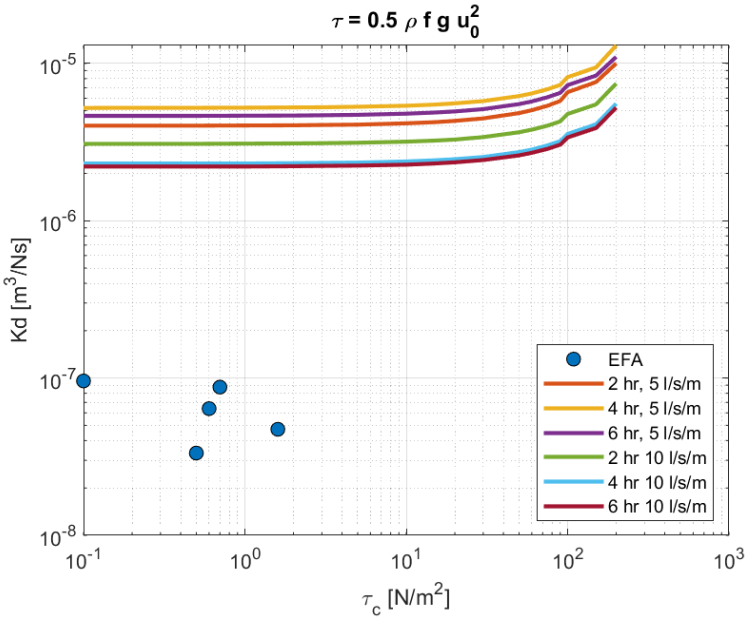

Figure A.2 Calibration results of the Delfzijl tests using $\tau=0.5\rho f g u_0^2$

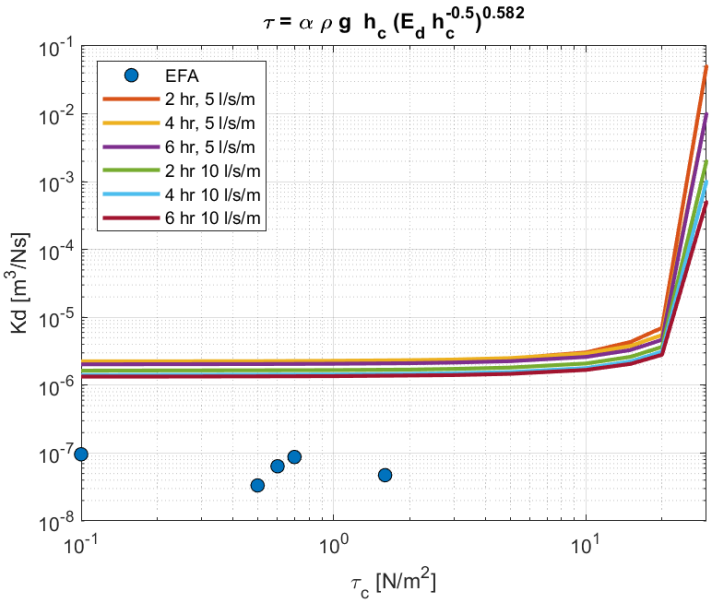

Figure A.3 Calibration results of the Delfzijl tests using the formulation of the ISL model for the shear stress.

B Additional information Delfzijl tests

Table B.1: The overtopping volumes released from the WOS during the simulated storms of the Delfzijl tests

1 l/s/m		**5 l/s/m**		**10 l/s/s**	
Volume (l/m)	Number of volumes in 6 hr (-)	Volume (l/m)	Number of volumes in 6 hr (-)	Volume (l/m)	Number of volumes in 6 hr (-)
50	54	50	225	50	384
150	54	150	123	150	252
400	9	400	81	400	147
700	6	700	30	700	57
1000	3	1000	12	1000	33
		1500	3	1500	9
		2000	3	2000	6

Table B.2 The erosion profiles of the Delfzijl tests abstracted from Figure 3.2

	1 l/s/m	5 l/s/m			10 l/s/m		
X (m)	Y0-6 hr (m)	Y0-2 hr (m)	Y2-4 hr (m)	Y4-6 hr (m)	Y0-2 hr (m)	Y2-4 hr (m)	Y4-6 hr (m)
0.0	7.95	7.95	7.94	7.96	7.95	7.96	7.94
0.5	7.84	7.84	7.83	7.83	7.83	7.83	7.83
1.0	7.74	7.74	7.72	7.74	7.72	7.74	7.72
1.5	7.56	7.54	7.55	7.56	7.56	7.56	7.55
2.0	7.40	7.39	7.37	7.39	7.37	7.39	7.39
2.5	7.22	7.21	7.19	7.23	7.20	7.21	7.22
3.0	7.07	7.05	7.05	7.07	7.06	7.06	7.05
3.5	6.90	6.91	6.90	6.90	6.88	6.90	6.88
4.0	6.64	6.77	6.76	6.75	6.75	6.74	6.64
4.5	6.56	6.65	6.66	6.64	6.64	6.65	6.56
5.0	6.46	6.53	6.52	6.53	6.51	6.53	6.39
5.5	6.37	6.37	6.34	6.37	6.33	6.35	6.37
6.0	6.19	6.19	6.19	6.18	6.18	6.12	5.21
6.5	6.02	5.93	5.90	5.89	5.89	5.28	5.02
7.0	5.86	5.76	5.52	5.51	5.43	5.07	4.92
7.5	5.69	5.53	5.28	5.07	4.90	4.88	4.86
8.0	5.50	5.29	4.96	4.76	4.75	4.76	4.75
8.5	5.28	5.18	4.82	4.72	4.73	4.65	4.51
9.0	5.07	5.05	4.65	4.58	4.48	4.49	4.46
9.5	4.91	4.91	4.67	4.46	4.46	4.46	4.39
10.0	4.76	4.71	4.58	4.47	4.31	4.31	4.26
10.5	4.59	4.54	4.43	4.51	4.26	4.26	4.22
11.0	4.44	4.37	4.29	4.29	4.22	4.24	4.22
11.5	4.30	4.23	4.06	4.08	3.98	3.98	4.00
12.0	4.15	4.10	3.81	3.80	3.75	3.75	3.75
12.5	3.97	3.95	3.78	3.79	3.68	3.68	3.57
13.0	3.76	3.76	3.76	3.77	3.57	3.43	3.42

3D erosion measurements have been performed for the Delfzijl case (Akkerman et al., 2007). The post-processing of the 3D erosion measurements were presented in Akkerman et al. (2007) resulting in the erosion profiles in Figure 3.2 and the figures presented in this appendix.

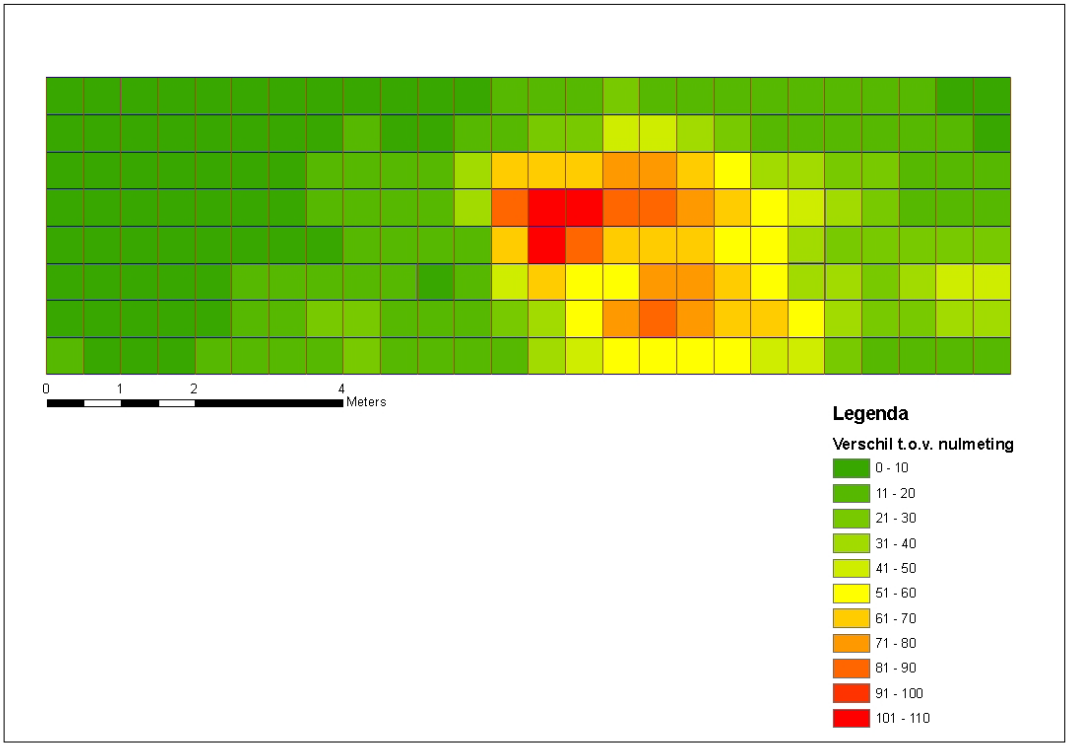

Figure B.1 The legend of the 3D erosion measurements at Delfzijl. The colours indicate the height difference relative to the baseline measurement in cm. The squares are 50 cm x 50 cm.

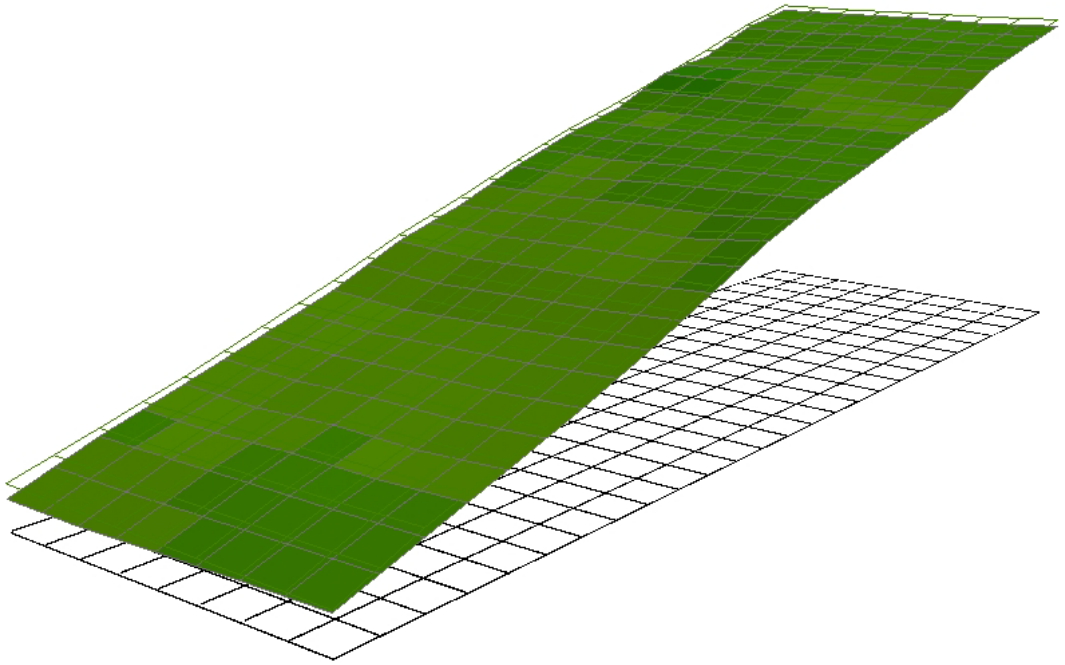

Figure B.2 The 3D erosion measurements after 6 hours 1 l/s/m of the Delfzijl case (for legend see Figure B.1)

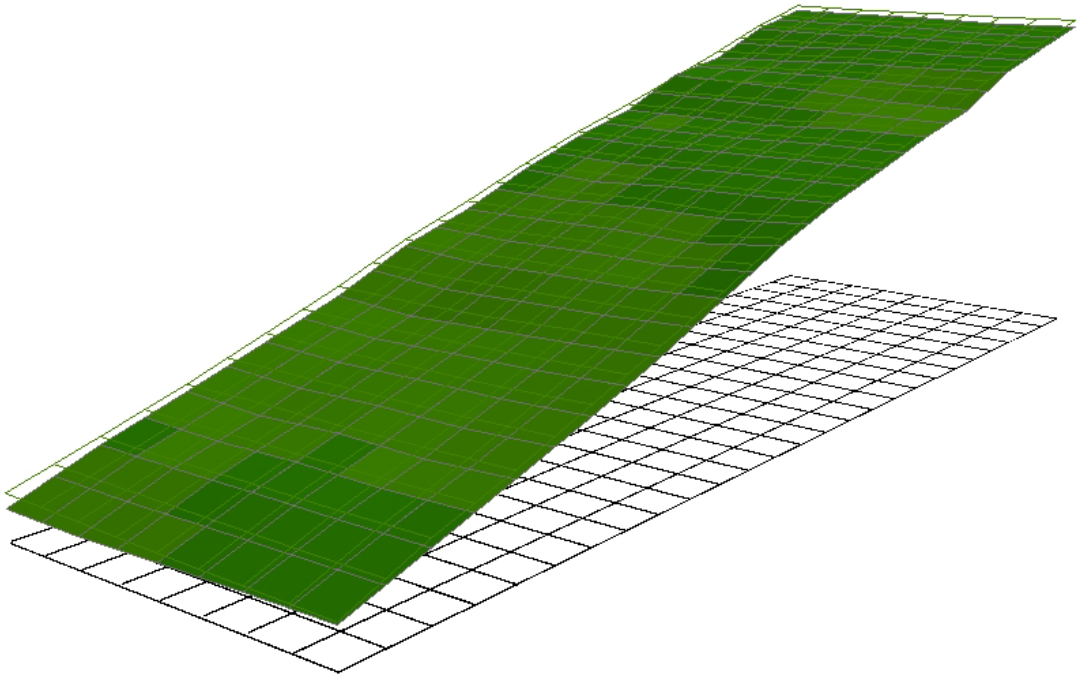

Figure B.3 The 3D erosion measurements after 2 hours 5 l/s/m of the Delfzijl case (for legend see Figure B.1)

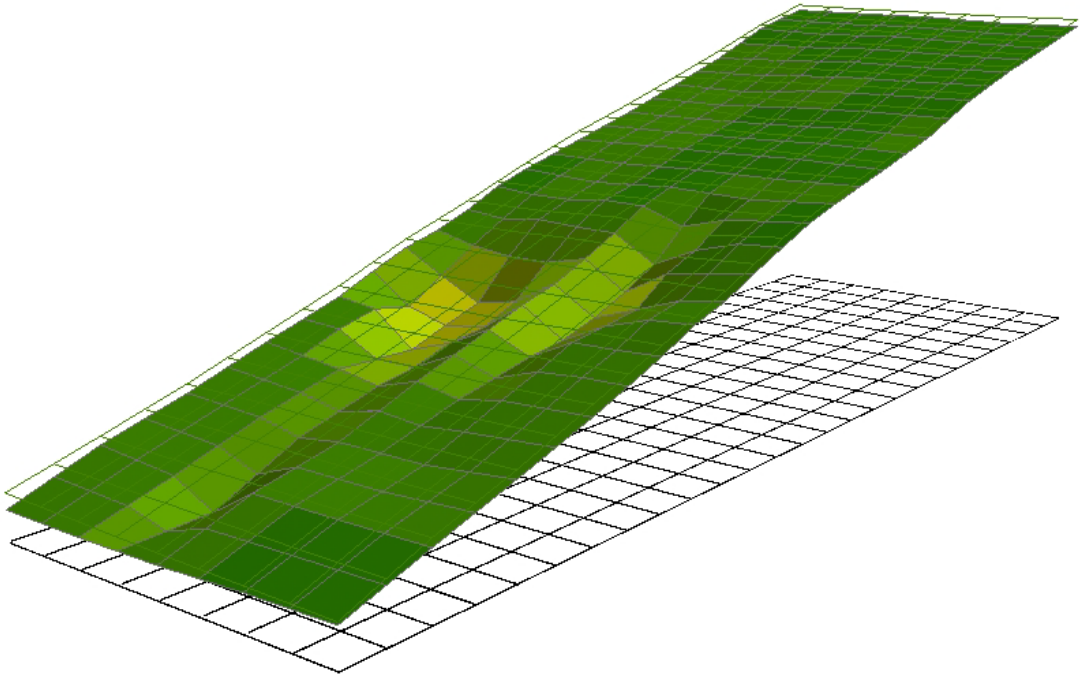

Figure B.4 The 3D erosion measurements after 4 hours 5 l/s/m of the Delfzijl case (for legend see Figure B.1)

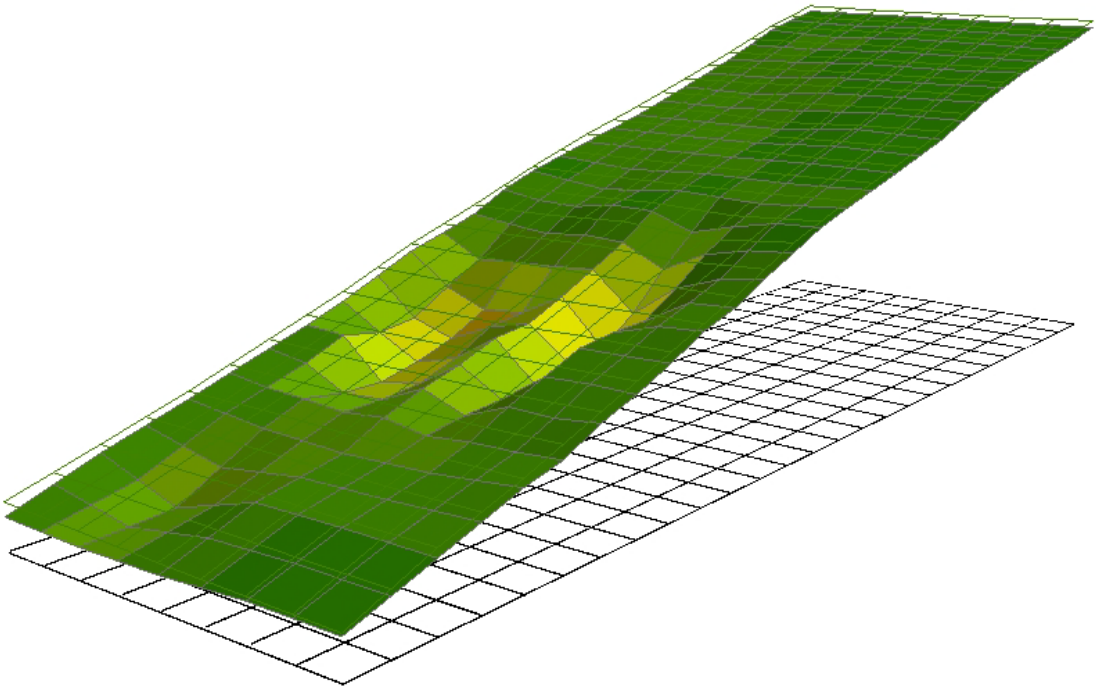

Figure B.5 The 3D erosion measurements after 6 hours 5 l/s/m of the Delfzijl case (for legend see Figure B.1)

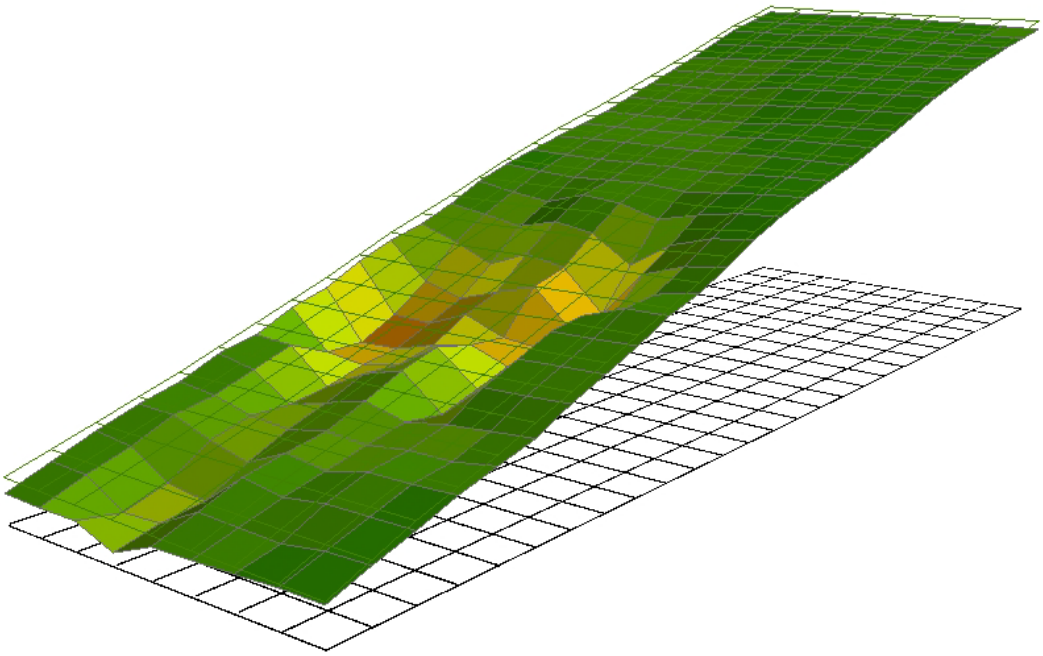

Figure B.6 The 3D erosion measurements after 2 hours 10 l/s/m of the Delfzijl case (for legend see Figure B.1)

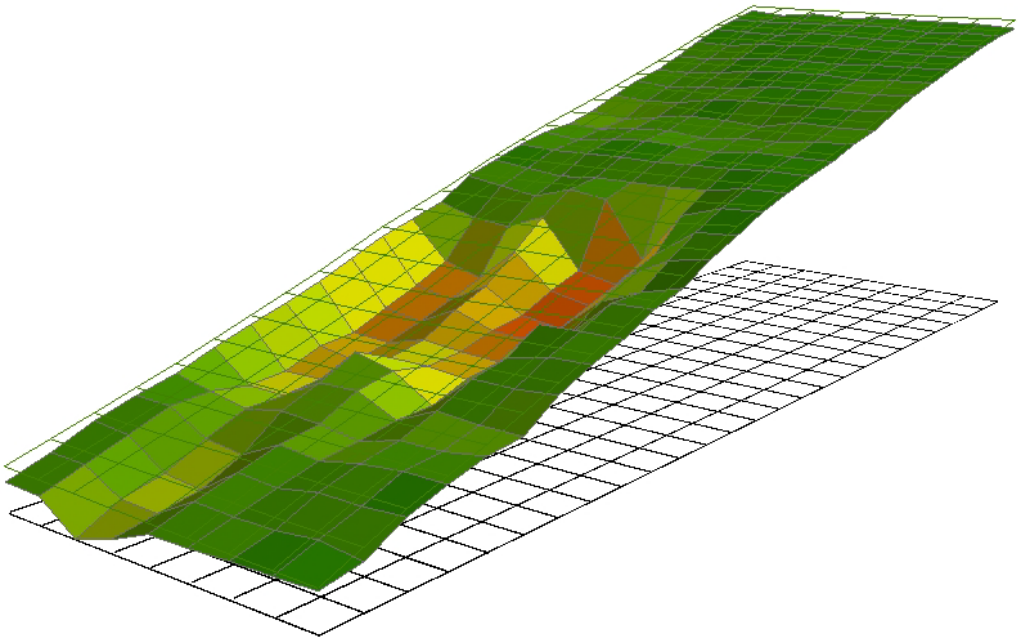

Figure B.7 The 3D erosion measurements after 4 hours 10 l/s/m of the Delfzijl case (for legend see Figure B.1)

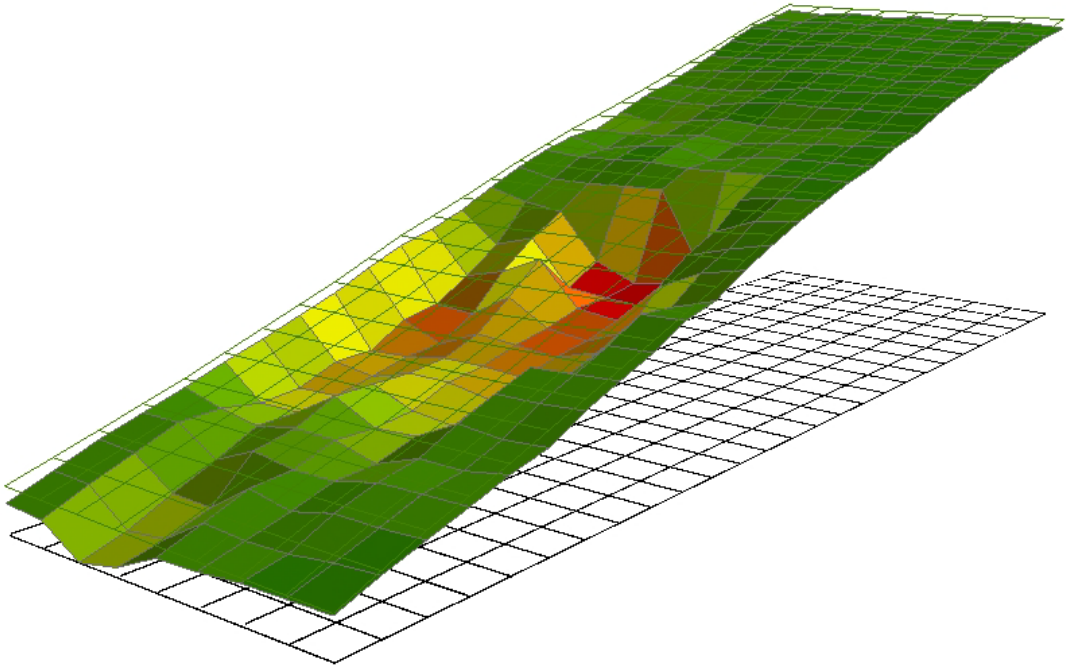

Figure B.8 The 3D erosion measurements after 6 hours 10 l/s/m of the Delfzijl case (for legend see Figure B.1)

C Additional information Polder2Cs tests

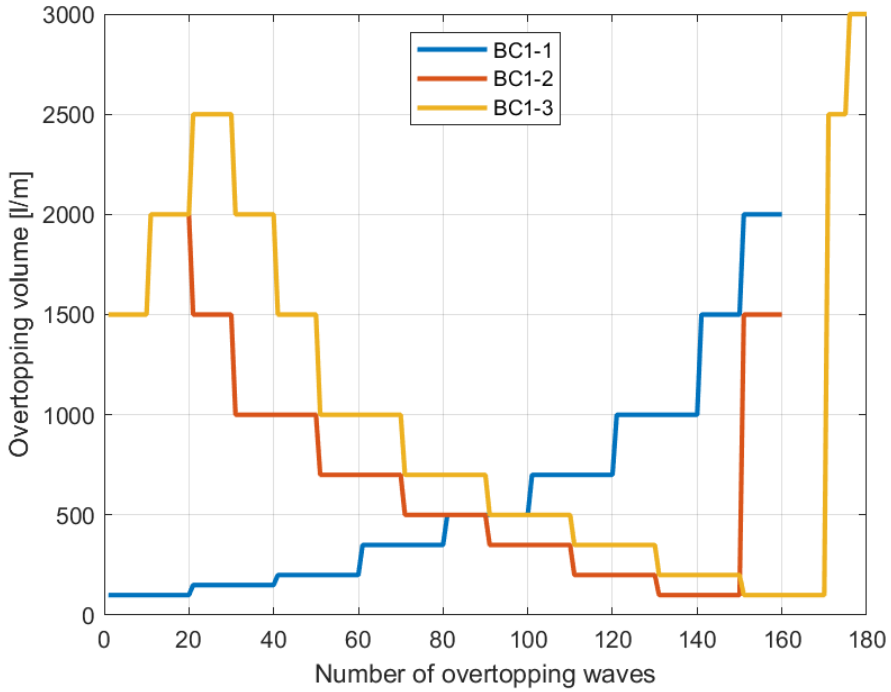

Figure C.1 Wave overtopping volumes released during the Polder2Cs tests with regular waves

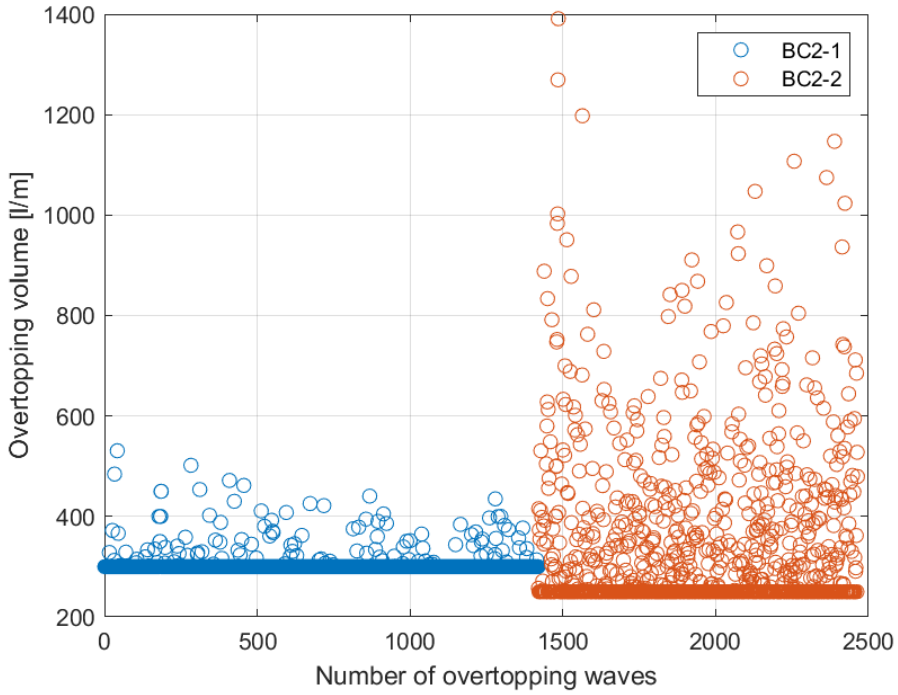

Figure C.2 Wave overtopping volumes released during the Polder2Cs tests with irregular waves representative for a river regime (BC2-1) and sea regime (BC2-2).

D Post-processing of the IJsselmeerdijk EFA tests

Six samples of the boulder clay were collected near test section 0 and test section 3 (Figure 3.5) by Deltares on 6 December 2023 and sent to ESTP to perform the EFA tests (Koelewijn, 2024). The results of the EFA tests include the measured erosion rate for different flow rates and shear stresses (Bennabi, 2024).

Following the method described by Van Damme et al. (2023), the erodibility coefficient K_d is determined from a linear fit through the measurements of the erosion rate E_r and the shear stress τ. The individual measurements of the flow rate by Bennabi (2024) and the resulting fits for the erodibility coefficient can be seen in Figure D.1 to Figure D.6. A range for the critical shear stress was reported by Bennabi (2024) for each sample. The erodibility coefficient was determined for both the lower and upper limit of the critical shear stress resulting in a range of values for K_d (Table D.1). The unit of the erodibility coefficient determined from the fit is mm/hr/Pa, which is transferred to m3/Ns by dividing by 3.6×10^{-6}.

The coefficients of determination R^2 vary between 0.43 and 0.89 for the six samples. The R^2 of samples 2, 5 and 6 is smaller than the recommended value of 0.65 (Van Damme et al., 2023) and the figures show that the value of K_d determined from the fit could be an overestimation. Sample 6 contains roots, which could be an explanation for the high critical shear stress of this sample.

In this study, the values of the shear stress and erodibility coefficient are averaged per sample were used resulting in the values reported in Table 3.10.

Table D.1 The critical shear stress τ_c and the erodibility coefficient K_d determined from the results of the EFA tests on the IJsselmeerdijk samples (Bennabi, 2024)

Sample	Identification	τ_c (Pa)	K_d (mm/hr/Pa)	Figure
1	Silt soil with shells	0.3 - 0.7	0.35 - 0.36	Figure D.1
2	Sandy silt with shells	0.1 - 0.8	1.4 - 1.5	Figure D.2
3	Fine sand with chippings	1.5 - 1.8	0.083	Figure D.3
4	Fine sand with chippings	0.5 - 1.1	0.33 - 0.34	Figure D.4
5	Silt soil with chippings	0.5 - 0.8	0.2	Figure D.5
6	Silt soil with shells and roots	1.9 - 4.7	0.061 - 0.071	Figure D.6

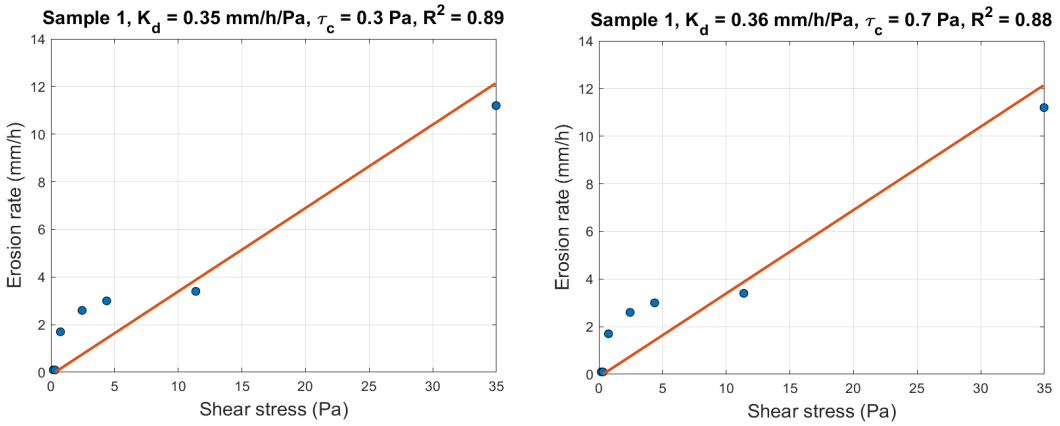

Figure D.1 Results EFA tests on sample 1 of the IJsselmeerdijken showing the measured erosion rates E_r and shear stresses τ together with the linear fit $E_r = K_d (\tau-\tau_c)$ and the coefficient of determination R^2

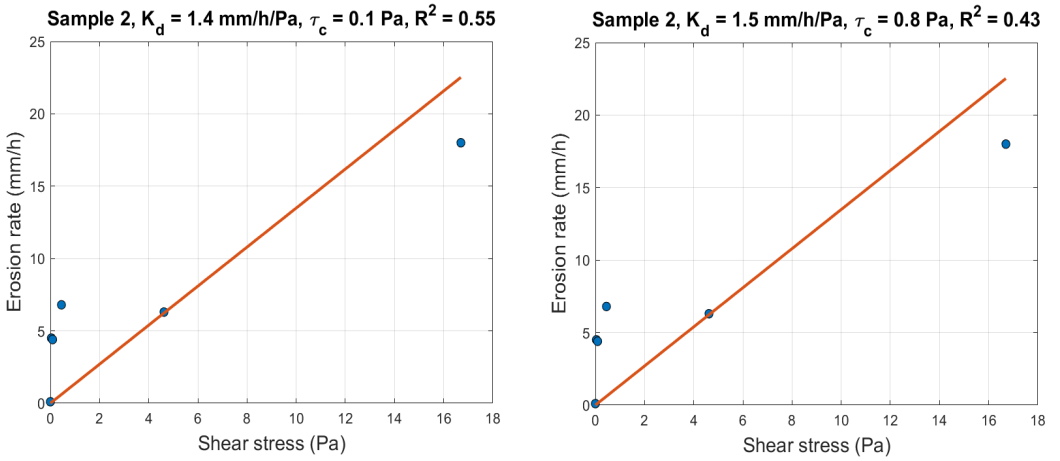

Figure D.2 Results EFA tests on sample 2 of the IJsselmeerdijken showing the measured erosion rates E_r and shear stresses τ together with the linear fit $E_r = K_d (\tau-\tau_c)$ and the coefficient of determination R^2

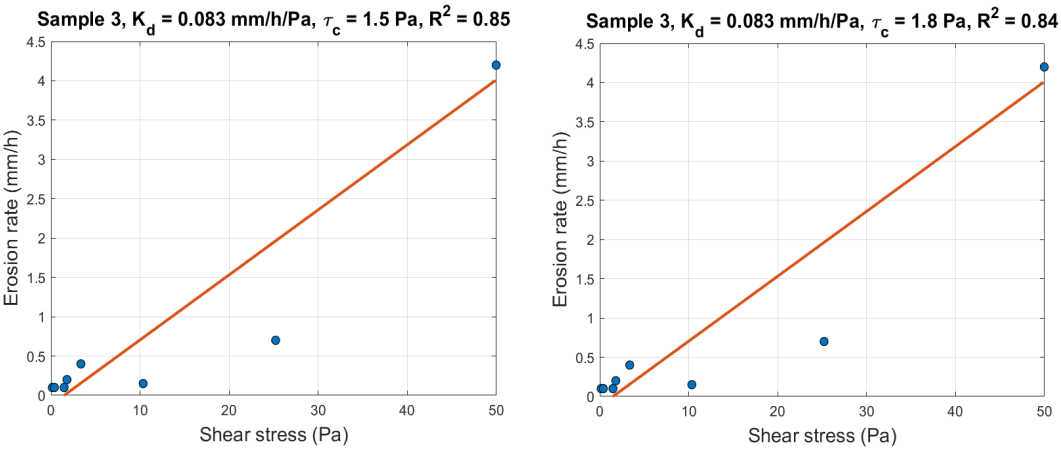

Figure D.3 Results EFA tests on sample 3 of the IJsselmeerdijken showing the measured erosion rates E_r and shear stresses τ together with the linear fit $E_r = K_d (\tau-\tau_c)$ and the coefficient of determination R^2

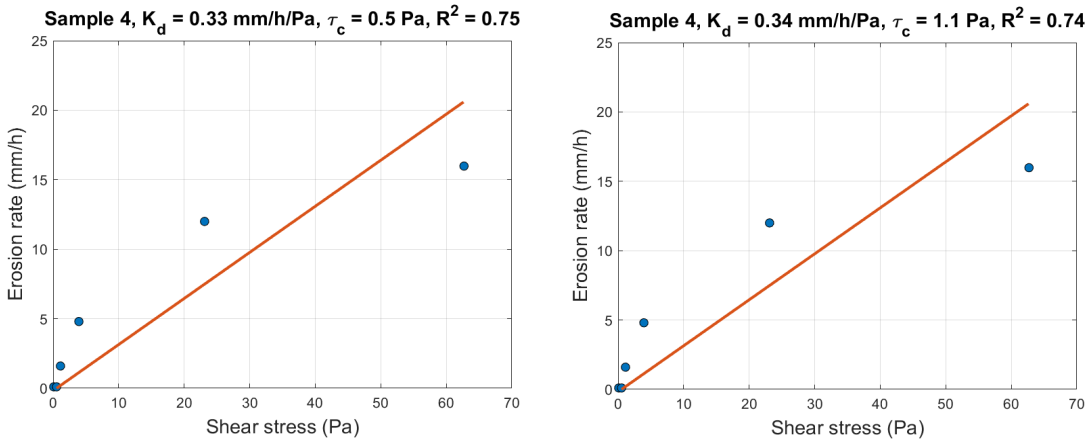

Figure D.4 Results EFA tests on sample 4 of the IJsselmeerdijken showing the measured erosion rates E_r and shear stresses τ together with the linear fit $E_r = K_d (\tau-\tau_c)$ and the coefficient of determination R^2

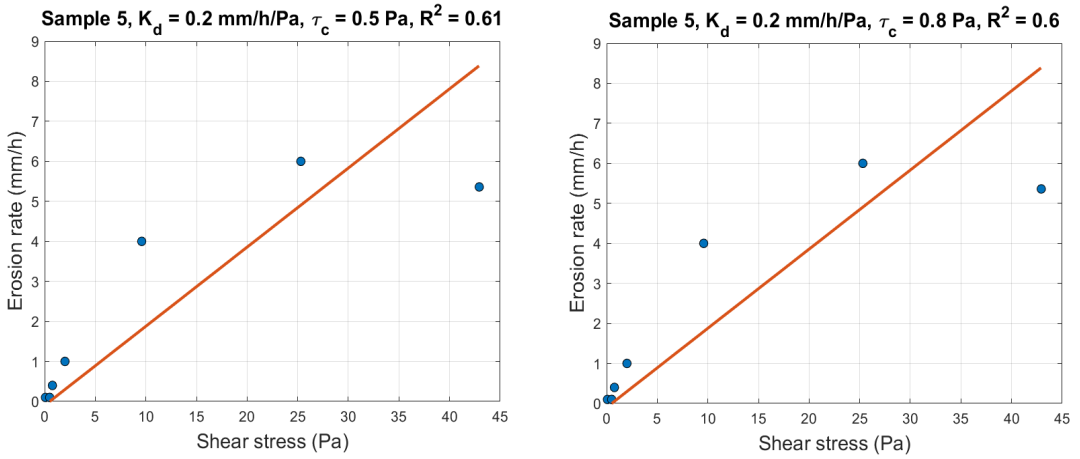

Figure D.5 Results EFA tests on sample 5 of the IJsselmeerdijken showing the measured erosion rates E_r and shear stresses τ together with the linear fit $E_r = K_d (\tau-\tau_c)$ and the coefficient of determination R^2

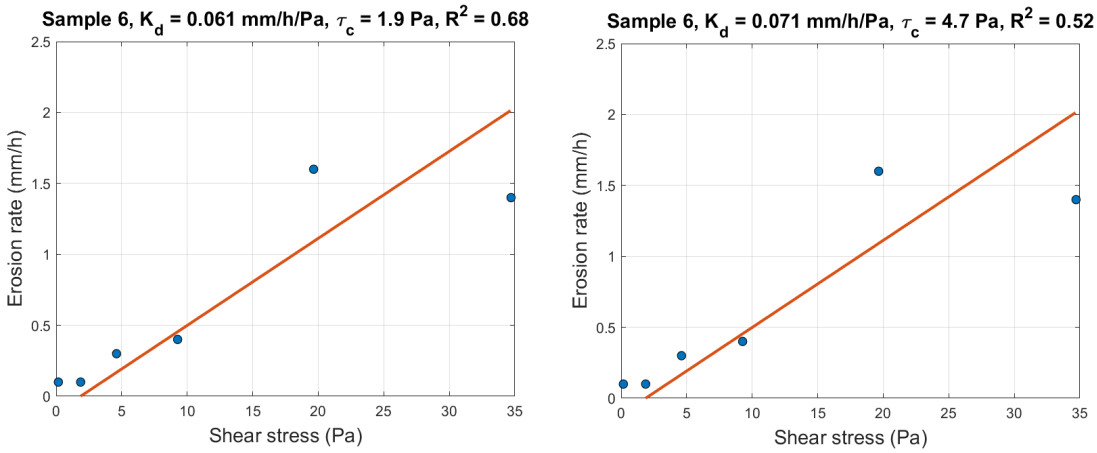

Figure D.6 Results EFA tests on sample 6 of the IJsselmeerdijken showing the measured erosion rates E_r and shear stresses τ together with the linear fit $E_r = K_d (\tau-\tau_c)$ and the coefficient of determination R^2

Deltares is an independent institute for applied research in the field of water and subsurface. Throughout the world, we work on smart solutions for people, environment and society.

Deltares

www.deltares.nl